U.S. DEPARTMENT OF LABOR MSHA
00029506

OFR 159-81
PB82-137326
[redacted]

High Concentration Dust Monitor

National Mine Health & Safety Academy
Technical Information Center & Library

U.S. Bureau of Mines
Twin Cities Research Center
LIBRARY

OFR
81-159

GCA/TECHNOLOGY DIVISION

DISCLAIMER NOTICE

The views and conclusions contained in this document are those of the authors and should not be interpreted as necessarily representing the official policies or recommendations of the Interior Department's Bureau of Mines or of the U. S. Government.

50272-101

REPORT DOCUMENTATION PAGE	1. REPORT NO.	2.	3. Recipient's Accession No.
4. Title and Subtitle: High Concentration Dust Monitor			5. Report Date: June 1981 6.
7. Author(s): Pedro Lilienfeld			8. Performing Organization Rept. No.
9. Performing Organization Name and Address: GCA Corporation GCA/Technology Division 213 Burlington Road Bedford, MA 01730			10. Project/Task/Work Unit No. 11. Contract(C) or Grant(G) No. (C) H0308010 (G)
12. Sponsoring Organization Name and Address: U.S. Bureau of Mines 400 Forbes Avenue Pittsburgh, PA 15213			13. Type of Report & Period Covered: Final Report 12/28/79-5/28/81 14.

15. Supplementary Notes

16. Abstract (Limit: 200 words)

The objective of this program was the development, design, fabrication and testing of a portable, self-contained prototype monitoring instrument capable of detecting and measuring airborne coal dust levels at concentrations in the range of 20 to 500 g/m^3. The output of the High Concentration Dust Monitor (HCDM) is essentially independent of particle size and composition, with a response time of 10 seconds. Direct concentration readout as well as internal memory or recording capabilities are incorporated in this device. The operation of the instrument is based on direct sensing of the mass concentration of airborne dust by air-path beta radiation attenuation. The monitor is battery operated and incorporates a microprocessor that controls periodic automatic zero referencing, executes the mass computations, records the data for subsequent playback, and performs internal diagnostic checks. The design emphasizes ruggedness, simplicity of operation, and adherence to intrinsic safety requirements.

This report covers the activities performed during the period of 28 December 1979 to 28 May 1981.

17. Document Analysis a. Descriptors

N/A

b. Identifiers/Open-Ended Terms

c. COSATI Field/Group

18. Availability Statement	19. Security Class (This Report)	21. No. of Pages
N/A	Unclassified	73
	20. Security Class (This Page): Unclassified	22. Price: ———

(See ANSI-Z39.18) See Instructions on Reverse

OPTIONAL FORM 272 (4-77)
(Formerly NTIS-35)
Department of Commerce

HIGH CONCENTRATION DUST MONITOR

Prepared for

UNITED STATES DEPARTMENT OF THE INTERIOR
BUREAU OF MINES

Prepared by

GCA CORPORATION
GCA/TECHNOLOGY DIVISION
BEDFORD, MASSACHUSETTS

FINAL REPORT FOR THE PERIOD
28 DECEMBER 1979 TO 28 May 1981

CONTRACT NO. H0308010

Author:

PEDRO LILIENFELD

Submitted June 1981

ABSTRACT

The objective of this program was the development, design, fabrication and testing of a portable, self-contained prototype monitoring instrument capable of detecting and measuring airborne coal dust levels at concentrations in the range of 20 to 500 g/m^3. The output of the High Concentration Dust Monitor (HCDM) is essentially independent of particle size and composition, with a response time of 10 seconds. Direct concentration readout as well as internal memory or recording capabilities are incorporated in this device. The operation of the instrument is based on direct sensing of the mass concentration of airborne dust by air-path beta radiation attenuation. The monitor is battery operated and incorporates a microprocessor that controls periodic automatic zero referencing, executes the mass computations, records the data for subsequent playback, and performs internal diagnostic checks. The design emphasizes ruggedness, simplicity of operation, and adherence to intrinsic safety requirements.

This report covers the activities performed during the period of 28 December 1979 and 28 May 1981.

FOREWORD

This report was prepared by GCA Corporation, Technology Division, 213 Burlington Road, Bedford, MA 01730 under USBM Contract Number H0308010. The contract was initiated under the Minerals Health and Safety Technology Program. It was administered under the technical direction of the Pittsburgh Research Center, Fires and Explosions Group with Kenneth L. Cashdollar acting as Technical Project Officer. William R. Mundorf and Michael L. Nowicki were the contract administrators for the Bureau of Mines. This report is a summary of the work recently completed as a part of this contract during the period December 28, 1979 to May 28, 1981. This report was submitted by the author in June 1981.

CONTENTS

	Page
Abstract	3
Introduction and background	6
Principle of operation and mass sensing design considerations	8
Measurement sensitivity and beta source selection	8
Beta radiation detector selection	12
Air density errors and their correction	13
Instrument development	15
Initial laboratory experiments	15
Flow characterization tests	23
HCDM design description	28
Inlet design and sampling considerations	28
Flow subsystem	31
Electronic subsystem	35
Panel controls	53
Error codes	53
Intrinsic safety and radioactive source licensing aspects	55
Instrument packaging and layout	56
Calibration check procedure	57
Final HCDM testing	59
Geiger tube high voltage tests	59
Instrument calibration tests	61
Zero concentration stability tests	68
Statistical measurement error determination	70
Environmental testing results	70
Conclusions and recommendations	73
References	74

ILLUSTRATIONS

1.	Relationship between range (maximum penetration) of beta rays and the absorption coefficient	10
2.	High concentration dust monitor layout/assembly	16
3.	HCDM Geiger detector interface and pulse shaper circuit, and frequency-to-voltage converter	17
4.	Experimental data of beta attenuation for HCDM sensing geometry	19
5.	Experimental setup for beta attenuation calibration of the HCDM using air-CO_2 mixtures	21
6.	Gas mixture calibration of the HCDM sensing system	22
7.	CO_2-Air calibration	24
8.	Test setup used to determine the effectiveness of the clean air curtain flows over the beta source and detector	26
9.	Photograph of the clean-air curtains made visible by means of cigarette smoke	27

ILLUSTRATIONS (continued)

		Page
10.	HCDM inlet configuration	29
11.	Aspiration efficiency for HCDM inlet, as function of ventilation speed and particle aerodynamic diameter	30
12.	Three-way flow valve developed for HCDM	33
13.	Flow system of HCDM	34
14.	Block diagram of electronic circuitry of the high concentration dust mass monitor	37
15.	Start routine logic flow diagram	39
16.	Check default value logic flow diagram	40
17.	Change constant routine logic flow diagram	41
18.	BDC entry routine logic flow diagram	42
19.	Measurement routine logic flow diagram	43
20.	Beta count routine logic flow diagram	44
21.	Log routine logic flow diagram	45
22.	Binary fraction routine logic flow diagram	46
23.	Update memory routine logic flow diagram	47
24.	Playback routine logic flow diagram	48
25.	Error routine logic flow diagram	49
26.	Schematic diagram	51
27.	Schematic diagram	52
28.	Layout of front panel of HCDM	54
29.	Beta count rate vs voltage for two detectors	60
30.	Mass readouts for simulated concentration of 20 g/m^3	62
31.	Mass readout for equivalent concentration of 475 g/m^3	63
32.	Mass readouts for simulated concentration of 75 g/m^3	64
33.	Calibration of HCDM using Mylar absorbers	65
34.	Final CO_2-air calibration set up	66
35.	CO_2-Air calibration results	67
36.	Dust comparison tests	69
37.	Zero-concentration beta counting rate stability test results	71

TABLES

1.	Accuracy as a function of mass concentration	11

SECTION 1

INTRODUCTION AND BACKGROUND

The potential danger of explosion and its propagation in underground coal mines arises principally from three sources: methane gas, coal dust deposited on the surfaces of the mine, and airborne coal dust. The prevention of such conflagrations requires periodic monitoring of those three potential factors. Methane detectors are in widespread use, and various methods are employed and are presently being developed to determine the incombustibility of deposited coal and rock dust mixtures. Monitoring of airborne coal dust concentrations at the potentially explosive level has not received as much attention due to the lack of adequate instrumentation. Requirements for instrumentation capable of performing such measurements have been defined based on recent investigations on the flammability of coal dusts.[1] It is interesting to note that potentially dangerous levels of many airborne combustible dusts are only weakly dependent on the type of combustible dust; i.e., similar minimum concentrations are required to maintain and propagate a conflagration whether the material is coal, grain, or sugar.[2] Thus, typical values of the order of 50 to 150 g/m^3 appear to be characteristic of minimum levels required for potential explosions. Particle size influences coal dust explosibility: smaller sizes increase the chances for such explosions. However, as the average coal dust particle diameter becomes smaller than about 50 μm the effect of size is diminished; i.e., the lean flammable limit depends only on the mass concentration and is insensitive to particle diameter for the smaller sizes, thus justifying mass concentration sensing approaches to characterize potentially dangerous levels.

The objective of this program was the development, design, fabrication and testing of a portable, self-contained monitoring instrument capable of detecting and measuring airborne such potentially explosive coal dust levels at concentrations in the range of 20 to 500 g/m^3. The output signal provided by this monitor is designed to be essentially independent of particle size and composition, with a response time of the order of 10 seconds. Direct concentration readout as well as internal memory capabilities were incorporated in this device. The design emphasizes ruggedness, simplicity of operation, and adherence to intrinsic safety requirements.

The sensing method incorporated in this monitoring instrument is based on direct; i.e., in situ, beta absorption detection across an air gap of the order of a few centimeters using a very low energy beta-emitting isotope. The measurement system includes automatic periodic referencing in order to

compensate for any air density fluctuations and/or detector drifts. Measurements, directly indicated in g/m^3, are updated automatically every 10 seconds.

The monitor incorporates a microprocessor whose functions are to control the automatic control sequences required for the measurement as well as to perform the required computations and diagnostic indications.

A detailed description of the various elements of the instrument are presented within the main body of this report which covers the activities performed during the period of 28 December 1979 to 28 March 1981.

SECTION 2

PRINCIPLE OF OPERATION AND MASS SENSING DESIGN CONSIDERATIONS

The measurement of very high mass concentrations of airborne particulates poses a unique challenge to the instrumentation designer in that, although sensitivity requirements may not be demanding, the usual particle collection-based approaches for mass sensing are seriously affected by rapid overloading of the required collection surfaces. Filtration, impaction, electrostatic precipitation (the latter one having been ruled out in this case because of its inherent danger as a potential explosion trigger) all are applicable to the mass monitoring of respirable and/or ambient concentration levels but become impractical at the typical concentrations of the order of 100 g/m^3 to be sensed within the present application.

The approach developed within this program, based on beta attenuation sensing, is a definite departure from the usual configurations incorporating that technique. It is based on direct; i.e., in situ, beta absorption detection across an air gap of about 2 centimeters using a very low energy beta-emitting isotope. The measurement system includes automatic periodic referencing in order to compensate for any air density fluctuations and/or detector drifts. Measurements, directly indicated in g/m^3, are updated automatically every 10 seconds.

This overall approach permitted the incorportion of such functions as unattended operation, continuous recording, and alarm output signals. The monitor incorporates a miniature microprocessor whose functions are to: control the automatic control sequences required for the measurement, perform the required mathematical computations, control the display of mass concentration and of diagnostic indications, and control data recording as well as subsequent data playback for unattended monitoring.

Measurement Sensitivity and Beta Source Selection

In this section a discussion is presented on the theoretical principles controlling the design of the in-situ beta attenuation airborne particulate sensing configuration, the geometrical design criteria, measurement sensitivity and beta source selection criteria.

The beta attenuation measurement sensitivity or limit of detection can be defined by:[3]

$$E_r\% = \frac{100\ \sqrt{2}}{\mu_m\ C\ d\sqrt{N_o}} \qquad (1)$$

where E_r is the relative standard deviation in percent, μ_m is the mass absorption coefficient (source isotope dependent), C is the mass concentration of dust to be measured, d is the distance between source and detector (i.e., the air gap), and N_o is the initial or reference beta count.

Equation 1 can be derived as a practical approximation of the rigorous equation:[4]

$$E_r\% = \frac{100}{\mu_m\delta\ \sqrt{N_o}} \left(1 + e^{\mu_m\delta}\right)1/2 \qquad (2)$$

where δ, the mass per unit area, is equal to the product Cd of Equation 1. For small variations in absorber thickness, as in the present case; i.e., when δ is small and thus $e^{\mu_m\delta}$ is near unity, Equation 2 can be approximated by Equation 1. From inspection of Equation 1 it can be concluded that for a given source isotope (μ_m) and a given mass concentration (C), there are only two parameters that can be varied in order to achieve the required measurement sensitivity (E_r). These two parameters are the air gap (d) and the detected beta count (N_o). The beta count is limited by detector characteristics and the activity of the source, and the air gap is limited by the penetration or range of the beta radiation (energy dependent). Figure 1 shows the relationship of beta radiation range; i.e., the maximum mass/area that can be penetrated, and the absorption coefficient which defines the sensitivity of the attenuation; i.e., the decrease in detected radiation due to a given absorber mass/area. In practice, the total sum of all absorbing elements between the source and detector should not exceed about one-half of the range value for a given isotope. Thus, in order to increase the gap, to increase measurement sensitivity, higher beta energy emitting isotopes must be used, thus reducing the value of μ_m correspondingly, as indicated by the curve of Figure 1. In other words, E_r of Equation 1 is really limited by the product $\mu_m d$ which is nearly constant over a wide range of beta energies. This criterion, however, must be modified by a very important geometrical consideration. The amount of radiation received by the beta detector is, among other factors, dependent on the solid angle subtended by the source at the detector. For given source and detector dimensions an increase in air gap results in a decrease of the solid angle, thus requiring additional source activity or an increase of overall dimensions. Therefore, in order to minimize sensor dimensions and source activity, while maintaining the required measurement sensitivity, the air gap should be as small as possible; i.e., of the order of a few centimeters. Air, at standard pressure and temperature, has a mass/area = 1.23 d (mg/cm^2), where d is the air gap in centimeters. The minimum practical detector window thickness corresponds to about 1 mg/cm^2 which obviously rules out the use of Hydrogen-3 (Tritium) as indicated by Figure 1. The next practical source isotope is Nickel-63 with a

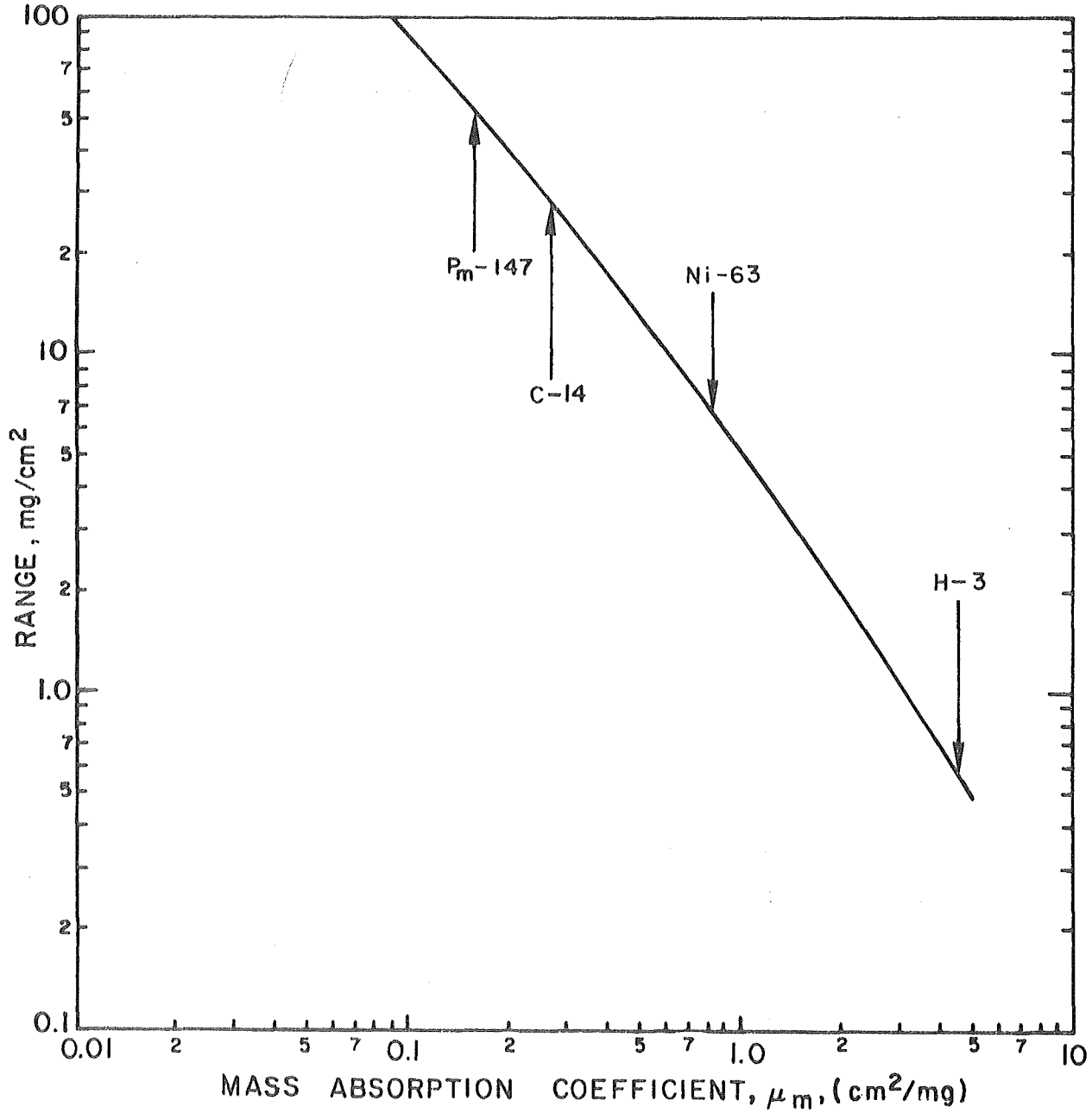


FIGURE 1. - Relationship between range (maximum penetration) of beta rays and the absorption coefficient (characteristic values of those parameters are indicated for four relevant beta-emitting isotopes).

range of about 6.7 mg/cm^2, which corresponds to a total practical absorber mass/area of 6.7/2 = 3.4 mg/cm^2. Of this, a minimum of 1 mg/cm^2 is required for the detector window, leaving 2.4 mg/cm^2 for the air gap which corresponds to a distance d = 2 cm.

Returning to Equation 1 we obtain that for a Nickel-63 source (μ_m = 0.81 cm^2/mg), a value of d = 2 cm, a mass concentration C = 50 g/m^3, E_r = $\pm$ 20 percent, the required beta count N_o becomes:

$$N_o = 2\left(\frac{100}{E_r\ \mu_m\ C\ d}\right)^2 = 2\left(\frac{100}{20 \times 0.81 \times 50 \times 10^{-3} \times 2}\right)^2 = 7600 \qquad (3)$$

For a response time of 10 seconds, and at a conservative count rate of 2500 sec^{-1} (for a Geiger-Muller tube) a total count of 25,000 can thus be obtained, which when replaced back into Equation 1 yields a relative standard deviation of about 11 percent at the mass concentration of 50 g/m^3. Table 1 summarizes the one-standard deviation intrinsic measurement accuracy, over the entire range of interest, based on the above selected parameters, using Equation 2.

TABLE 1. - Accuracy as a function of mass concentration (based on μ_m = 0.81 cm^2/mg, d = 2 cm, and N_o = 25,000 counts)

Mass concentration (g/m^3)	20	50	100	150	500
Accuracy (one sigma)	28%	11%	5.8%	3.9%	1.4%

The next step was to calculate the approximate amount of Nickel-63 activity required at the beta source in order to generate a maximum count rate of 10,000 sec^{-1} at the detector using a typical detection geometry. The amount of source activity, R, in millicuries can be calculated from:(3)

$$R = \frac{4\pi f}{3.7 \times 10^7 \times \eta_s \times \eta_d \times \theta \times \exp(-\mu_m\ \delta_T)} \qquad (4)$$

where f = the count rate at the detector (sec^{-1})

η_s = the source efficiency factor

η_d = the detector efficiency (not including window attenuation)

θ = the solid angle of detection, and

δ_T = the sum total of the mass/area of all absorbers between the source material and the active volume of the detector.

The source efficiency factor for Nickel-63 is relatively high (considering its very low energy) because it can be obtained as a diretly electroplated surface on a metal foil or plate substrate. Typical values for η_s are of the order of 0.5 to 0.75 for specific activities of 12 mCi/mg and surface plating densities of the order of 0.3 mg/cm^2.

Geiger-Muller detection efficiencies are of the order of 0.5. Based on a source-to-detector separation of 2 cm, an effective circular detection area of 6.8 cm^2, and a circular source area of 1.2 cm^2 we obtain $\theta = 0.53\pi$ sterad.

Based on a total absorber mass/area of 5 mg/cm^2 (including a high dust concentration); and replacing the above values in Equation 4 one obtains:

$$R \cong 0.46 \text{ millicurie}$$

Because of reasons of availability, and because for low energy beta emitters the activities calculated on the basis of Equation 4 are usually an underestimate, a 4 mCi Ni-63 source was obtained and incorporated in the instrument.

Although carbon-14 was considered as a possible alternative beta source isotope for this application, Ni-63 was selected because its lower energy permits the use of a smaller sensing gap, the radioactive material is mechanically more stable and rugged, and the surface uniformity with which Ni-63 sources can be manufactured is far greater than for C-14 sources. This latter characteristic is important in achieving an essentially exponential beta attenuation behavior.

The selected beta source isotope, Nickel-63, is commercially available as an electroplated source onto a platinum foil (1.25 cm diameter and 0.005 cm thick). This configuration ensures complete mechanical integrity and stability (the foil is cemented to an aluminum support disc). Nickel-63 has a half-life of 96 years, and the maximum beta energy emitted by that isotope is 66 keV. Nickel-63 is a pure beta emitter which, by its beta radiation, decays into a stable; i.e., nonradioactive isotope (Cu-63). A 4 millicurie source with the above cited dimensions was obtained from New England Nuclear (North Billerica, Mass.).

Beta Radiation Detector Selection

Two types of beta radiation detectors were considered for this instrument development: (a) a "pancake" type Geiger-Muller tube, and (b) a silicon partially depleted solid-state detector. The decision was made, within the initial design phase, to incorporate the Geiger-Muller tube rather than the silicon detector, because of ready availability, lower cost, ruggedness, and the relative simplicity of the associated circuitry.

During the initial phase of this program contact was established with a Geiger-Muller manufacturer (TGM, Inc., Waltham, Mass.) in order to obtain an especially designed tube with a minimum-thickness mica window reinforced by

means of a thin metallic grid. Although several attempts were made by TGM to develop such a device, materials failures prevented that organization from succeeding in their endeavor. In lieu of that approach, TGM then provided to GCA a standard "pancake" detector with a 1.5 mg/cm^2 window. Experimental evaluation indicated that this type of detector would be entirely satisfactory for this application, and the sensing-flow chamber, to be described in detail further on, was then designed to incorporate that detector.

Another type of beta detector that was evaluated within this program was a silicon partially depleted sensor. These devices are usually applied to the detection of gamma radiation, although they have been used for both alpha and beta sensing. These semiconductor detectors are the counterpart of scintillation detectors in that they provide energy-dependent outputs which, by means of pulse-height analysis, are used to obtain energy spectra of radioactive sources. The present application, however, is based on total beta counting and thus, one of the principal characteristics of these detectors is not utilized. The only important advantage of silicon detectors over G-M tubes in their application to beta counting resides in their far shorter dead-time which permits counting rates up to about 10^6 sec^{-1} (for Ni-63 betas). Disadvantages of these detectors are, however, relatively high cost, lack of ruggedness and somewhat greater complexity of the auxiliary circuitry. It was considered, nevertheless, that a cursory evaluation of these detectors would be desirable.

Within this project, a solid state beta detector was obtained on approval from the manufacturer. The device was a Princeton Gamma-Tech model PD-300-24-300M Surface Barrier Detector, with its ancillary preamplifier. The tests were rather inconclusive since the detector failed to operate properly, and was returned to the manufacturer. The preliminary conclusion reached was that these types of devices are too delicate for this application. In addition, cost and complexity of auxilliary circuitry are additional negative factors to be considered. It was then decided that no further tests of semiconductor detectors would be performed within this program, in view of the above mentioned experience, and based on the successful performance of the pancake-type geiger tubes.

Air Density Errors and Their Correction

The principal potential sources of error for a beta detection system as described above are: (a) variations in air density, and (b) deposition of dust on the source and/or detector surfaces. The latter problem and its prevention will be discussed within the design description. The former factor will now be considered. The air density-related measurement error, $\varepsilon\rho$, can be defined as:

$$\varepsilon\rho = \frac{\Delta\rho}{\Delta t} \times t_r$$

where $\Delta\rho/\Delta t$ is the rate of change of air density, and t_r is the period of time between consecutive reference beta or zero-dust correction measurements.

The principal environmental factors affecting the air density are barometric pressure and temperature fluctuations. Typical maximum barometric pressure changes result in $\Delta\rho/\Delta t$ values of the order of 0.05 g/m^3 per minute. Temperature changes in mines could be expected to reach maximum rates of 10°C/hour which corresponds to a $\Delta\rho/\Delta t$ of about 0.7 g/m^3 per minute. Thus, in order to maintain this latter error contribution (i.e., the largest factor affecting air density) to less than 10 percent at the minimum level of the range of mass concentrations of dust (i.e., 20 g/m^3), a reference or zero compensation must be performed about every 3 minutes, thus resulting in a maximum value of $\varepsilon\rho = 2$ g/m^3, at the above extreme temperature rate of change. The description of the actual method of implementation of this zero correction will be presented further on within this document. This compensation approach consists, in essence, of automatic periodic flushing of the sensing chamber by means of clean air, the determination of the zero dust concentration beta transmission, and the incorporation of this reference count in the computation of subsequent concentration measurements, until a new zero reference count is obtained and updated in the electronic memory of the instrument.

SECTION 3

INSTRUMENT DEVELOPMENT

Within this section of the report a summary description and the results of the developmental testing performed on the High Concentration Dust Monitor (HCDM), prior to its final configuration, will be presented. The first step in this development effort consisted of the design and fabrication of a sensing-flow chamber to be used as a test configuration to evaluate and optimize the beta mass sensing, and air flow pattern aspects of the system. Figure 2 depicts the salient design characteristics of the sampling-sensing-flow configuration incorporated in the HCDM and subjected to extensive testing during all phases of the program.

Initial Laboratory Experiments

Two general types of experiments were performed during the early phases of this program: (1) beta sensing characterization tests, and (2) flow pattern characterization tests. Each of these will be discussed in some detail.

Beta Sensing Tests

In order to perform the series of tests required to characterize the beta sensing system an interface electronic driver-detection circuit was assembled and interconnected with a laboratory bench-top high-voltage power supply. In addition, a pulse-shaping and frequency-to-voltage converter circuit was designed and assembled whose objective was to permit analog strip chart recording of the beta detector output for calibration and long term stability tests. Figure 3 is a schematic diagram of this circuit. The pulse shaping section of that circuit was later incorporated in the electronic circuitry of the completed HCDM.

As expected, the detected count rate was in excess of the design characteristics of the Geiger tube (because of the relatively high activity of the available Ni-63 source). In order to reduce the detected beta count rate to acceptable levels, as well as to determine the actual beta attenuation characteristics of the detection configuration, a slide-in frame was designed and fabricated, to support the thin Mylar films of known mass/area used for this purpose. Two different film thicknesses were used: 0.15 and 0.25 mil, equivalent to 3.8 and 6.4 μm which in turn correspond to 0.522 and 0.858 mg/cm^2 as determined experimentally by weighing a known area of each of the two films.

3/8 X 1/4
ALU

H
(AMATON

E
(ADALET

FR

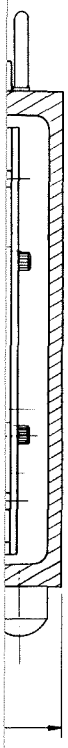


FIGURE 2.

UNLESS OTHERWISE SPECIFIED ALL DIM. ARE IN INCHES TOLERANCES .X ± .06 .XX ± .02 .XXX ± .005 ANGLES MACHINE FINISH ✓ BREAK SHARP EDGES AND COR. .005 TO .020R APPROX	DR J MC NULTY DATE CHK 4-7-80 APPROVALS RELEASED	GCA/TECHNOLOGY DIVISION BURLINGTON ROAD, BEDFORD, MASSACHUSETTS 01730 / PHONE 617-275-9000
MATERIAL USED ON ATION	FINAL FINISH	TITLE HIGH CONCENTRATION DUST MONITOR LAYOUT/ASSEMBLY SIZE E DRAWING NO. 1-391-1000 SCALE FULL WT SHEET 1 OF 1 REV

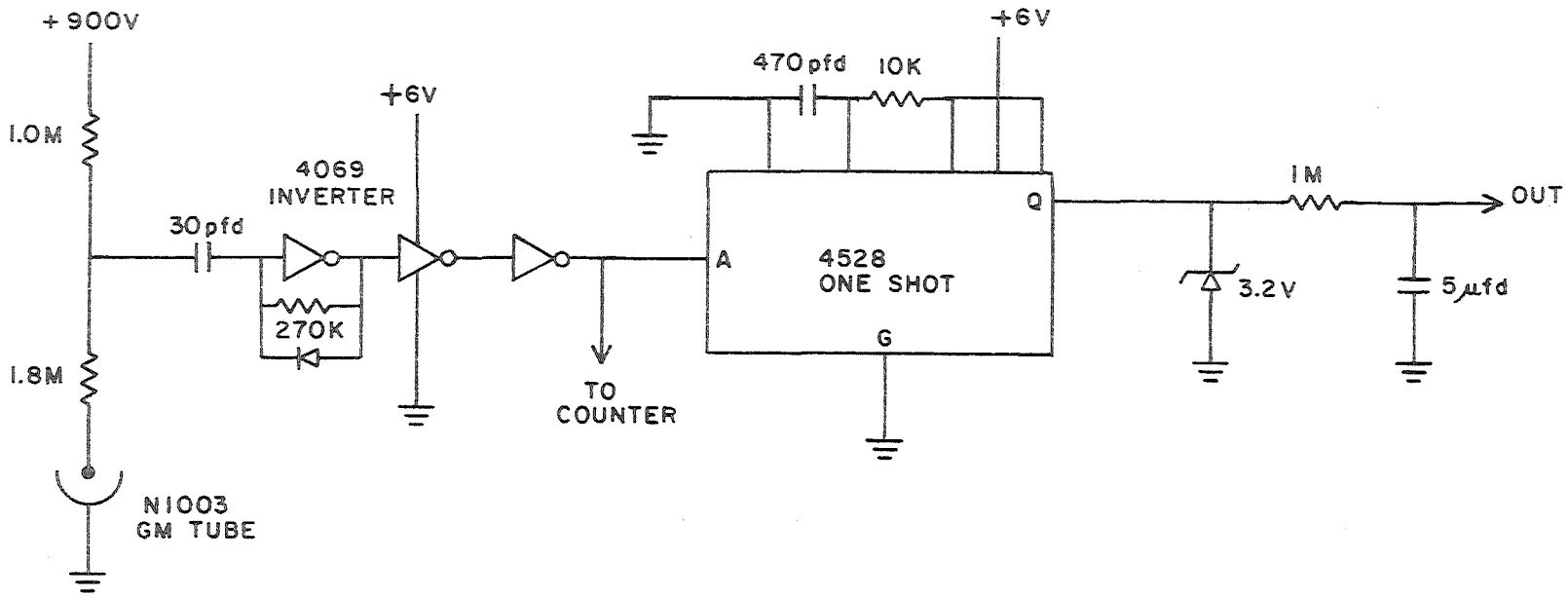


FIGURE 3. - HCDM Geiger detector interface and pulse shaper circuit, and frequency-to-voltage converter.

In practice the physical source-detector separation of 2 cm does not constitute the actual detection gap because a fraction of this distance is taken up by the two clean air curtains flowing over the source and detector surfaces. It was initially estimated that the effective sensing gap was about 1.5 cm rather than the physical separation of 2 cm, thus the two Mylar films mentioned above (0.15 and 0.25 mil thickness) were equivalent to 348 and 572 g/m^3.

The objective of these beta sensing characterization experiments were: (a) to determine the actual mass absorption coefficient (μ_m), (b) to establish the operating region of maximum exponential response linearity (i.e., linearity when plotted as a semilog graph), and (c) to determine the maximum beta count rate compatible with the Geiger tube selected for this application.

Figure 4 is a plot of the initial experimentally obtained data points of beta count rate versus the mass/area of Mylar film absorbers interposed between the source and the detector within the actual sensing chamber of the High Concentration Dust Monitor. The data points on the semilog plot follow a typical inverse S-curve, where the high-count rate flattening is due to count losses associated with detection coincidence, and the high mass/area flattening is caused by multiple scattering of betas as the range thickness is approached. The actual position of this inverted S-curve along the abscissa and its length depend on the activity of the beta source, i.e., a lower activity source would result in a shift to the left and a lengthening of the S, whereas a higher source activity would result in the opposite behavior.

The straight portion of the curve of Figure 4, i.e., the logarithmic portion, is the region within which the HCDM was then designed to operate. This region is bounded by the dashed lines of Figure 4. The extent required to cover the entire measurement range of 0 to 500 g/m^3 is thus indicated. In practice, the zero dust concentration point is obtained by means of a single permanently installed 0.25 mil Mylar absorber, which for the configuration incorporated in the prototype instrument results in a clean-air count rate of about 6000 to 8000 sec^{-1} (see Figure 4).

The mass absorption coefficient can be empirically derived from the slope of the linear portion of the curve of Figure 4. The value of μ_m is obtained from:

$$\mu_m = \frac{\ln f_o - \ln f}{\Delta\delta}$$

where f_o = the initial (clean air) beta rate

f = the attenuated beta rate

$\Delta\delta$ = is the increment of mass/area that causes a beta rate change of f_o to f.

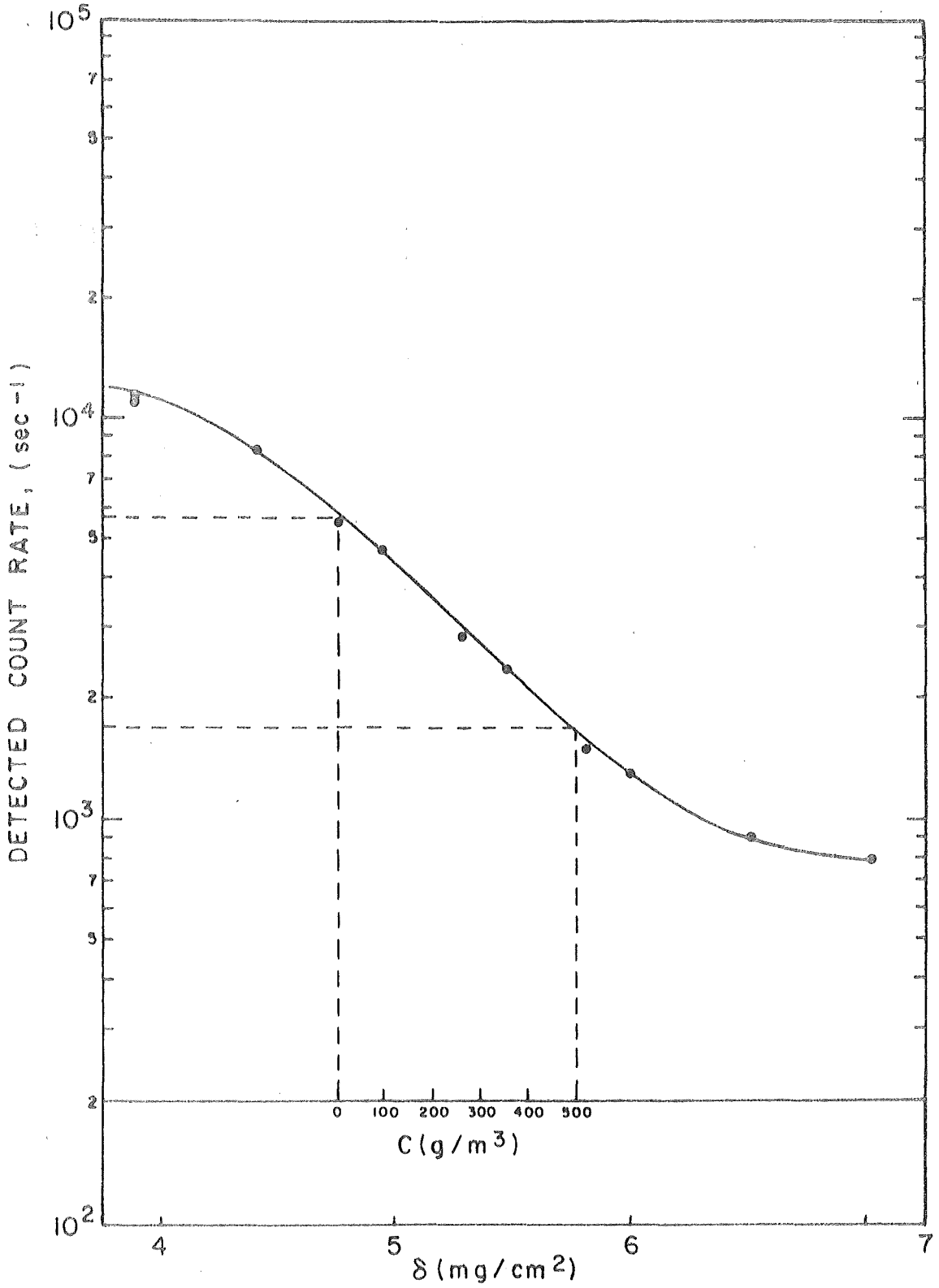


FIGURE 4. - Experimental data of beta attenuation for HCDM sensing geometry. Geiger Tube: TGM Type N1003. Beta Source: NEN 4mCi Ni-63.

For the curve of Figure 4,

$$\mu_m = \frac{\ln 5700 - \ln 1700}{5.75 - 4.75} \text{ cm}^2/\text{mg} = 1.21 \text{ cm}^2/\text{mg}$$

This value is higher than that indicated previously, i.e., 0.81 cm^2/mg, which is an average empirical value. For a given isotope, the sensing geometry, i.e., source and detector dimensions, their separation, as well as the spatial extent of the absorber are primary factors that influence the absorption coefficient.

The second series of tests, whose objective was to characterize the beta sensing configuration, was performed using a higher-than-air-density gas to simulate the presence of high dust levels within the sensing region of the HCDM. This method consists of introducing a known proportion mixture of air and the higher density gas into the sensor and varying that proportion while recording the resulting beta count rate. The gas selected for this experiment was CO_2 which has a density of about 1840 g/m^3 at room temperature, as compared to the density of about 1200 g/m^3 of air under the same conditions. Thus, by mixing the two gases a range of simulated dust concentrations from 0 to 640 g/m^3 (pure air to pure CO_2, respectively) was achieved.

The air-CO_2 experimental calibration setup is depicted in Figure 5. It should be mentioned that this method constitutes, in essence, an absolute calibration technique since it only relies on flow rate measurements to quantify the density within the sensing chamber of the HCDM. CO_2 was obtained from a pressurized tank and fed through a heat exchanger copper coil immersed in a water bath at room temperature in order to bring the CO_2 gas from the tank to that temperature. A flowmeter was recalibrated for CO_2, and the combined flow of air and CO_2 was allowed to mix in a 50 cc flask, as shown in Figure 5. A thermometer was used to ensure that the resulting gas mixture was at room temperature. Two separate pumps were used, one to draw the gas mixture through the sensing chamber, and the other to provide the clean-air curtain flows. The ratio of air and CO_2 was controlled by two needle valves and measured by means of the two inlet flowmeters shown in Figure 5. The clean-air curtain flow was metered separately.

Each data point was obtained by counting the detected beta pulses for 10 seconds on a digital frequency meter. The resulting data points are shown in Figure 6 for two different Geiger detectors subjected to this test.

The beta absorption coefficient, μ_m, derived from the two sets of data of Figure 6, for $\delta > 5.0$ mg/cm^2, averaged about 1.13 cm^2/mg (based on an effective sensing gap of 1.5 cm) which was only about 7 percent below the value obtained using Mylar film absorbers. These results served as mutual confirmation of the validity of both methods of calibration, i.e., the known mass/area plastic films, and the known gas mixture approach. One of the advantages of the gas mixture technique is that it does not require a prior assumption of a given sensing gap value; i.e., it is an absolute calibration independent of any geometrical considerations.

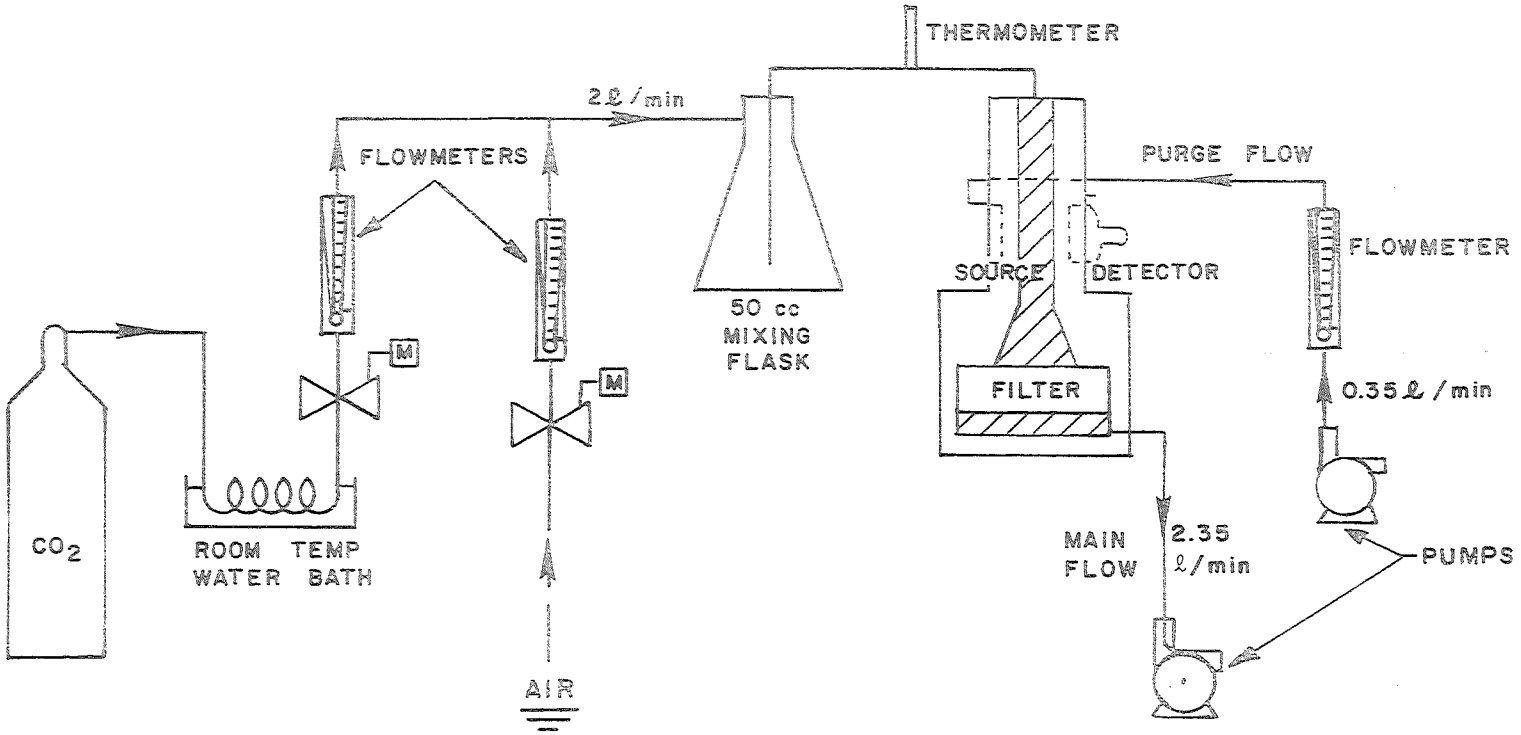


FIGURE 5. - Experimental setup for beta attenuation calibration of the HCDM using air-CO_2 mixtures.

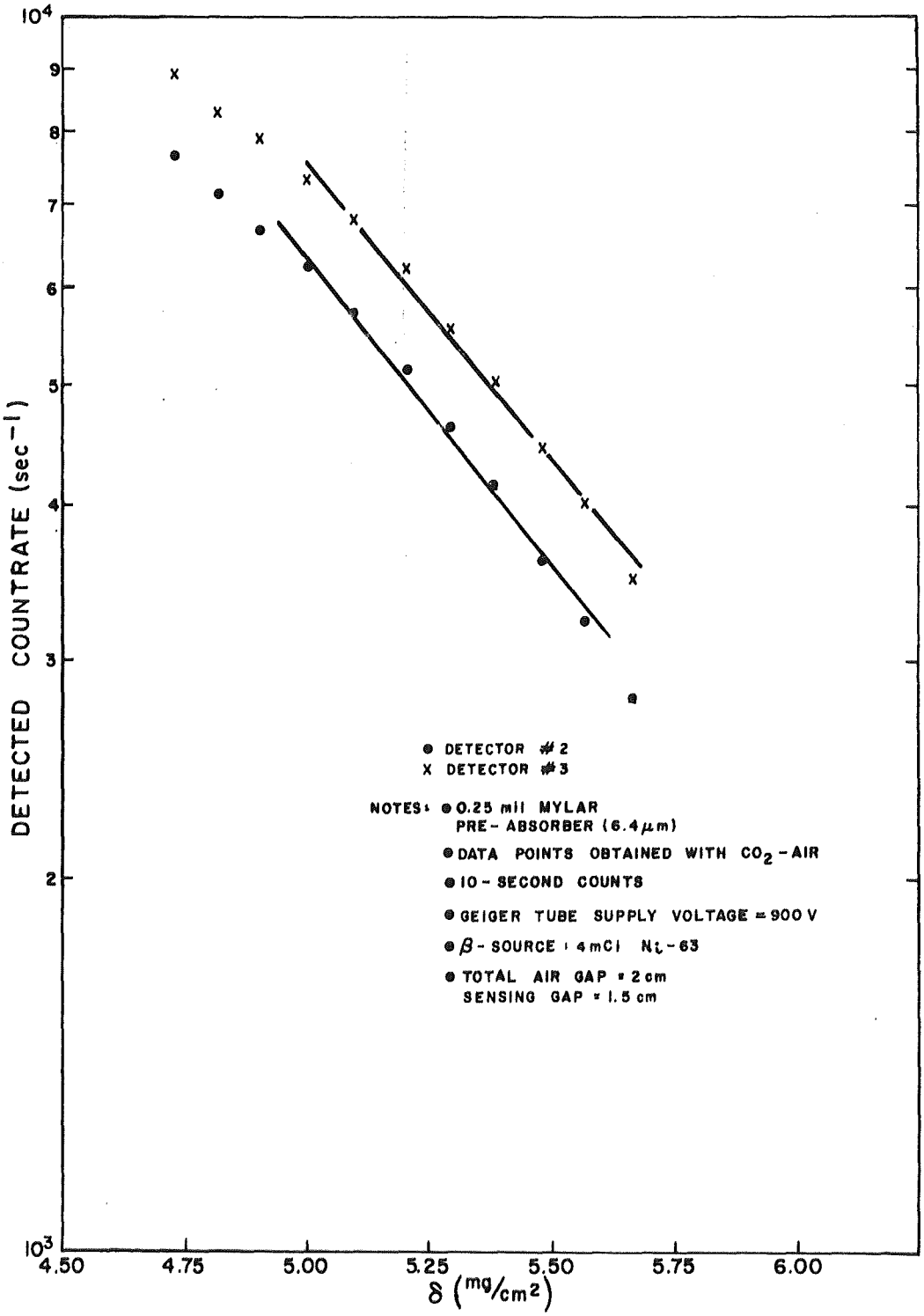


FIGURE 6. - Gas mixture calibration of the HCDM sensing system. (with pure air in flow curtains).

During the early phase of the experimental effort, it was observed that when the CO_2-air mixture was allowed to fill the entire gap between beta source and detector an essentially straight semilog response characteristic was obtained as this mixture was varied (see the steeper data line of Figure 7). However, when the gas mixture was constrained to the region between the air curtain sheaths, using only pure air for these curtain flows, a certain degree of curvature was observed. This curvature would have introduced a slight but perhaps acceptable error in the measurement. The different slopes between the full CO_2-air condition and the clean air sheaths condition are, of course, associated with the decreased width on the effective sensing gap of the latter case, a predictable behavior.

The actual mass absorption coefficient determined by the response to CO_2 with the gas mixture in the flow curtains was 1.19 cm^2/mg. Again, this agreed well with the μ_m factors previously determined by either the use of Mylar as an attenuator or by the CO_2-air mixture constrained to the sensing region. The curvature in the semilog plot shown in Figure 6 was later found to be the result of flow pattern irregularities between the clean-air curtain flows and the main central stream. The final CO_2-air calibration setup and the resulting calibration data are shown in a subsequent section of this report.

The experiments using the CO_2-air mixture method to simulate a controlled concentration of dust in the sensing region of the HCDM have supported and confirmed the extremely useful character of this approach. This technique is very similar to the nephelometer calibration method based on Freon-12 whose scattering intensity is known quite precisely. The CO_2-air method is straightforward and can be implemented with a minimum amount of standard laboratory hardware.

Flow Characterization Tests

One of the primary objectives of the initially performed flow tests was to determine the effectiveness of the clean-air flow curtains passing over the beta source and the detector surfaces and used to protect these from potential dust contamination. These clean-air curtains must be constrained to flow over the two surfaces without appreciably mixing with the primary stream of dusty air sampled from the environment. Careful geometric design of the channels, as well as matching of the air velocities of the dusty and clean air streams, are required to ensure flow parallelism and minimize interference between the two streams.

In order to determine experimentally that the design of the flow ducting configuration was capable of achieving the above objectives and in order to establish the proper flow rate relationships between the clean air flow rate and the primary sampling flow rate, an experiment was set up using cigarette smoke as a visual tracer. Rather than using this smoke to characterize the primary sample flow, it was concluded that this tracer should be injected into the clean-air curtain stream, thus permitting a clear visualization of the spatial extent and behavior of the sheath flows, which are the more critical aspects of the flow patterns within the beta detection region of the HCDM.

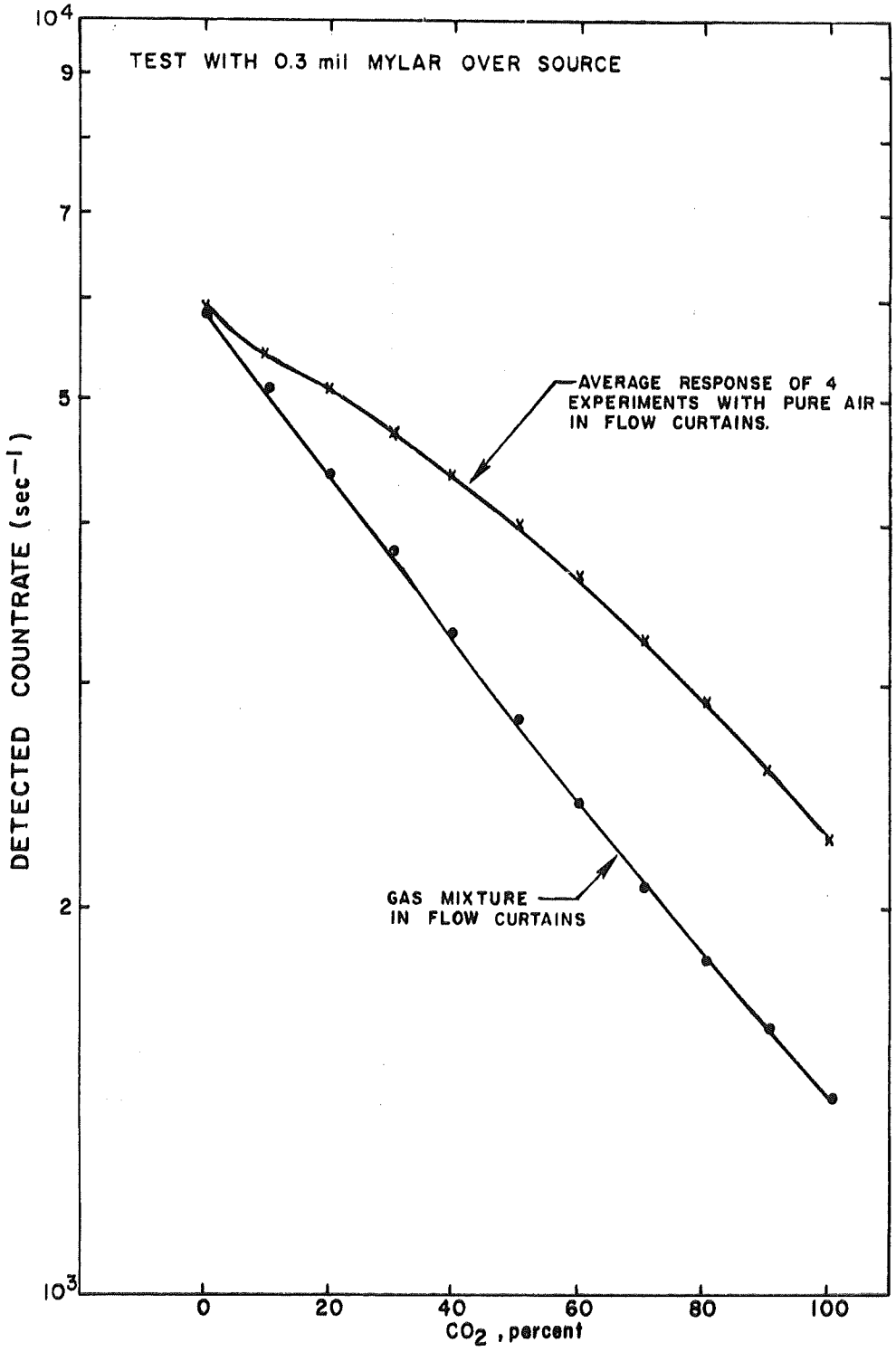


FIGURE 7. - CO_2-Air calibration.

The experimental setup used to perform the above described flow characterization is shown in Figure 8. Under normal operating conditions, a 2 l/min air flow rate enters the sample inlet, passes through a pleated filter, through the 3-way valve (in position 1 of Figure 8) and out through Valve A. Flow rate is measured at the system exhaust. Valve A is used to simulate the flow restriction which, in combination with the pressure sensor, will provide the signal to regulate the flow rate. Flow is regulated by pump voltage adjustment. From the output port of the pump, a small portion of the exhaust is diverted back into the sensing chamber to create the flow curtains over the beta source and detector. The flow curtain flow rate is regulated with Valve B.

To test the effectiveness of the flow curtains, the beta source and detector were replaced with transparent windows. Cigarette smoke was introduced into the curtain flow and observed by beaming a high intensity light source into one window. Observations were made through the other windows (to observe lateral spreading of the flow curtain across the source and detector) and from above the sample inlet (to determine the thickness and radial stability of the flow curtain).

It was found that adequate coverage of the beta source and detector was obtained at a flow curtain flow rate of 0.3 to 0.4 l/min, while keeping the thickness of the flow curtain at a minimum.

Figure 9, is a photograph of the curtain flow pattern made visible by means of cigarette smoke, using the experimental system described above and depicted in Figure 8. The photograph of Figure 9, was obtained by pointing the camera vertically downwards into the sensing chamber, after removal of the sampling inlet section. The white bands on either side of the oblong sensing cross section of Figure 9 represent the top views of the flow curtains which were illuminated by means of a perpendicular light beam passing through a transparent window installed in lieu of the beta source disc, as mentioned above. The multi-orifice background visible on that photograph is the inlet of a large capacity, replaceable pleated-filter cartridge, at the bottom of the sensing block.

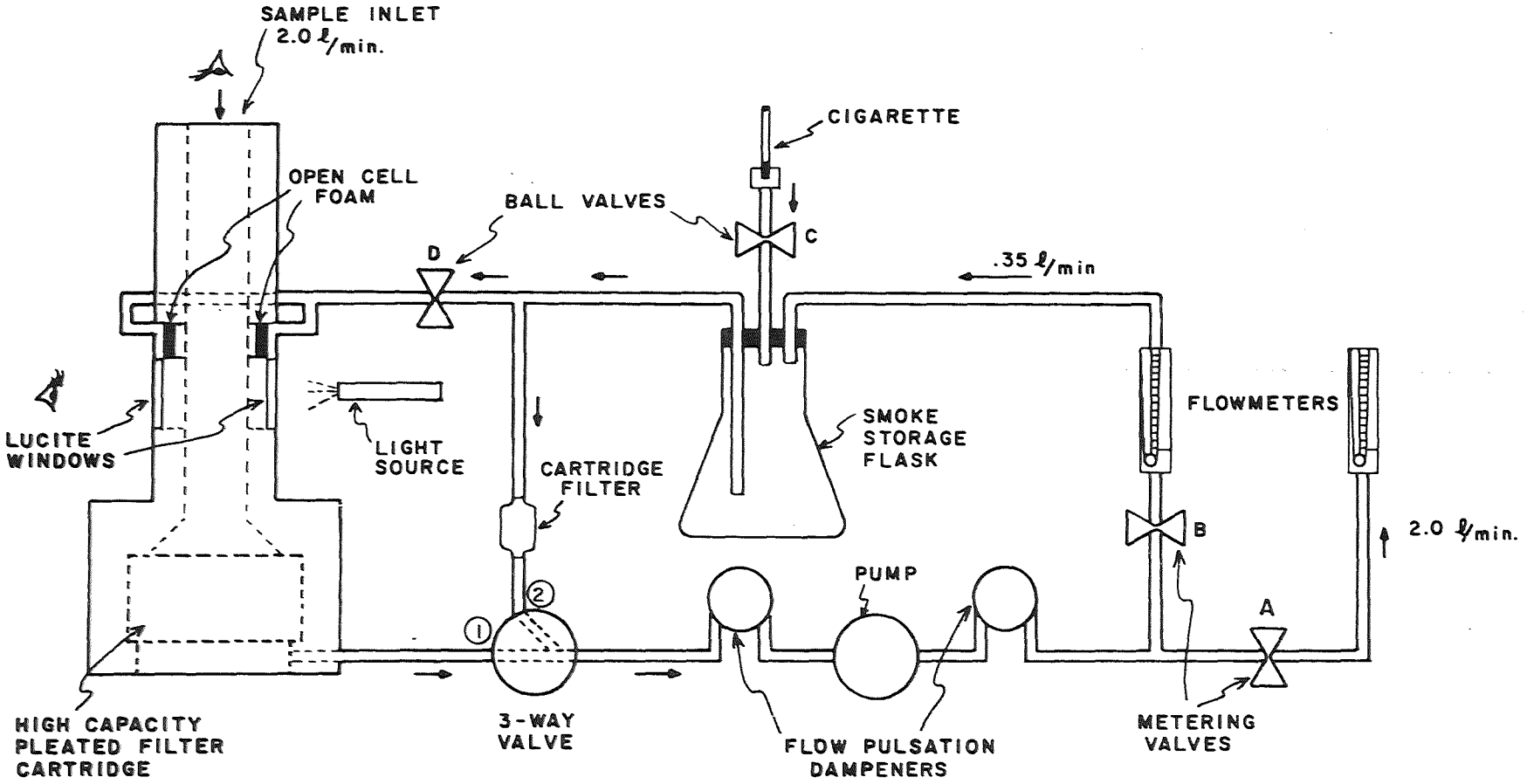


FIGURE 8. - Test setup used to determine the effectiveness of the clean air curtain flows over the beta source and detector.

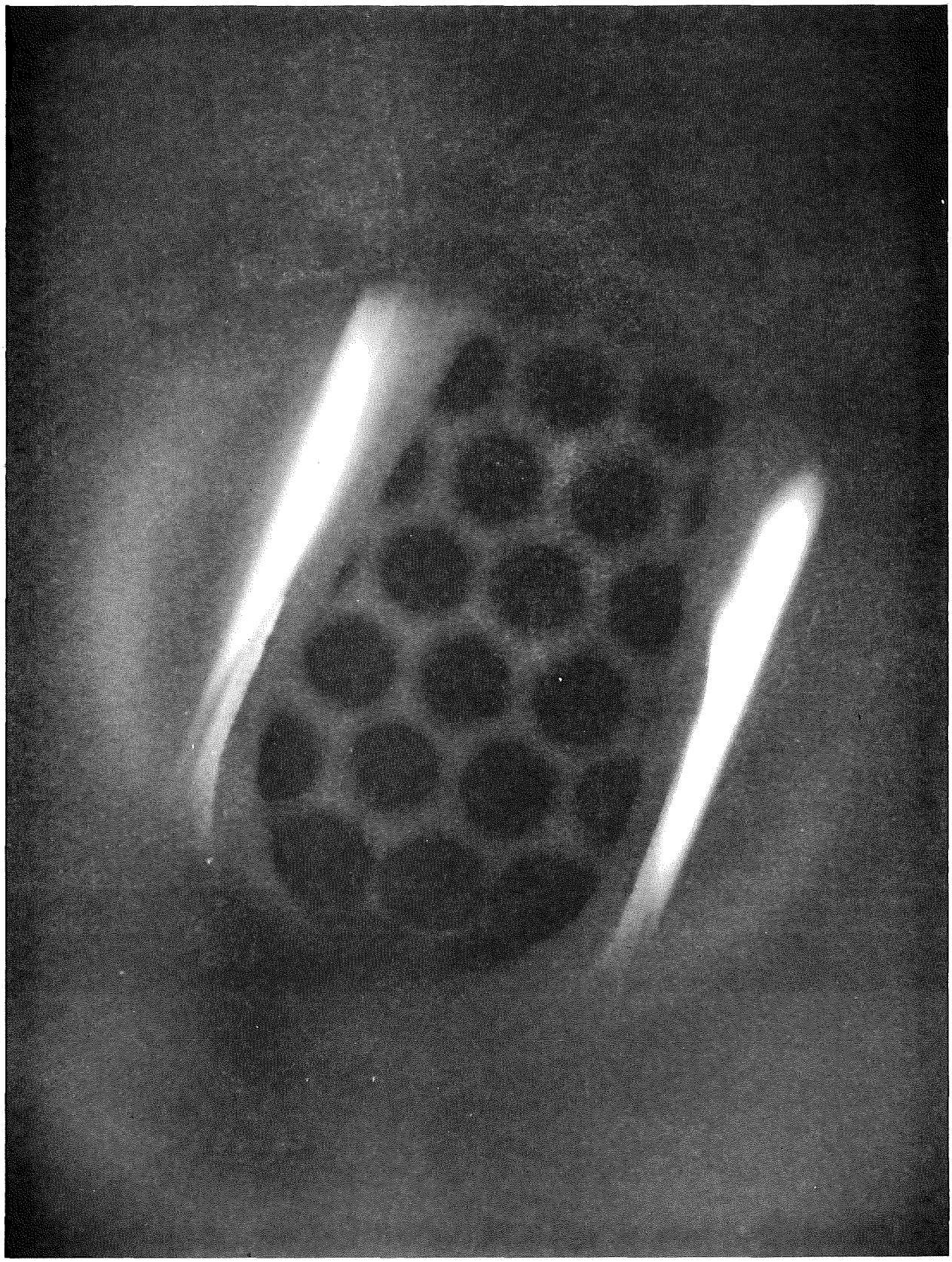


FIGURE 9. - Photograph of the clean-air curtains made visible by means of cigarette smoke. Central air flow rate was 2 lpm.

SECTION 4

HCDM DESIGN DESCRIPTION

Within this section of the report, a detailed description of the HCDM design will be presented. The discussion will be broken down as follows: (a) sample inlet and sensing duct design, (b) flow subsystem, (c) electronic subsystem, (d) instrument packaging and layout, and (3) intrinsic safety aspects.

Inlet Design and Sampling Considerations

The design of the inlet of the HCDM is a compromise between optimizing sampling efficiency and protecting the instrument from the entry of large debris and rocks. The type of inlet configuration selected for this application follows the general approach of a circular slit developed by two horizontal parallel surfaces (see Figure 10). The bottom surface is open and constitutes the sampling duct vertical entrance. This configuration is being advocated, as a general solution to the airborne particle sampling problem, by various investigators.[5,6]

We must assume that for some situations within which the HCDM is to operate, a significant horizontal air flow component will exist as a result of typical ventilation patterns. This type of free air motion will result in the transport of the dust to be measured across the vertical inlet to the HCDM, after having entered through the annular opening. Liu and Pui[5] applied Zebel's[6] treatment to this type of inlet and calculated the so-called "aspiration efficiency" as a functon of wind (i.e., ventilation) speed for various particle sizes. Figure 11 is a plot of the aspiration efficiency for the dimensions of the vertical inlet of the HCDM shown in Figure 1. It is obvious that at high ventilation speeds, and large particle diameters, i.e., above a few hundred feet per minute and for particle diameters exceeding about 50 μm, the aspiration efficiency drops rapidly. Clearly, removal of the top horizontal ducting plate above the inlet would not increase the aspiration efficiency if the predominant air motion is in the horizontal plane. At low ventilation speeds, however, the aspiration efficiency is high, even for particles as large as 80 μm. Two interchangeable inlet sections were designed for the HCDM: a short one (see Figure 10) to be used in those cases where spatial constraints exist, and a long version protruding about 25 cm above the upper surface of the HCDM enclosure. This latter inlet should be used whenever possible, in order to minimize free flow obstruction effects of the instrument case. The two types of inlet sections are readily interchangeable by means of the three thumb-screws shown in Figure 10.

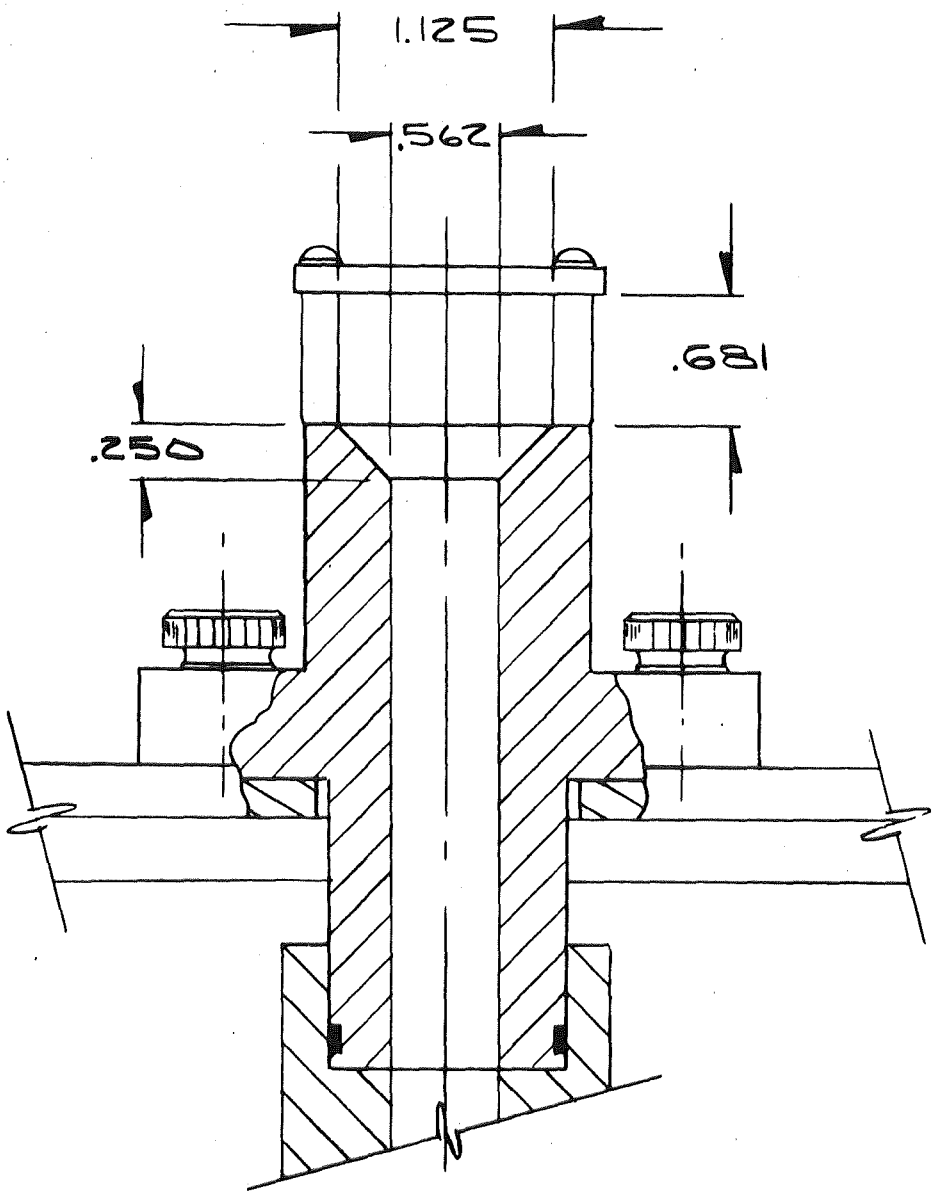


FIGURE 10. - HCDM inlet configuration (short version). Dimensions in inches.

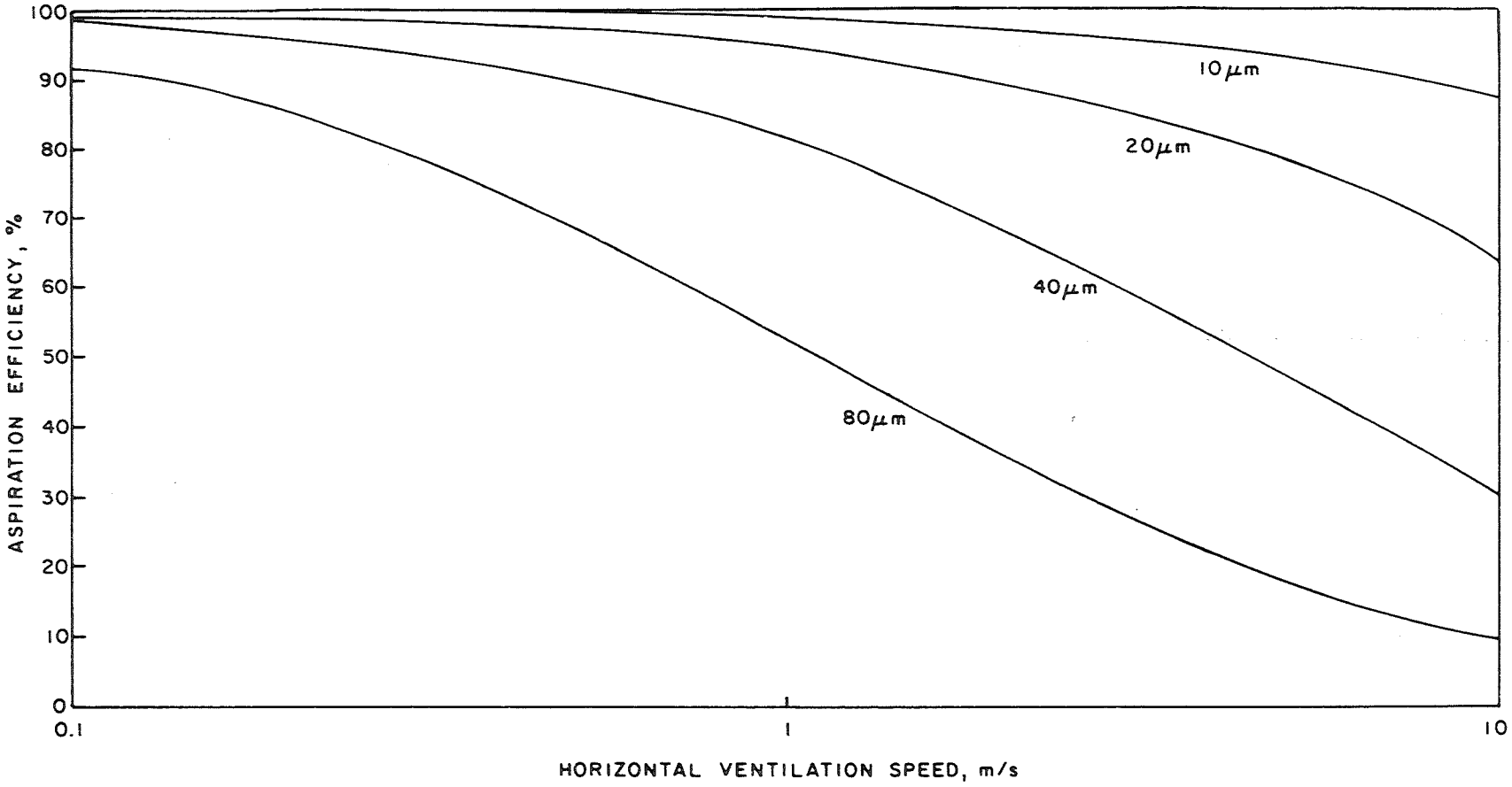


FIGURE 11. - Aspiration efficiency for HCDM inlet, as function of ventilation speed and particle aerodynamic diameter.

Through this section of this report, frequent reference will be made to Figure 2, which is a reduced engineering drawing of the internal layout of the HCDM, which shows, in cross section, the sample inlet and beta sensing chamber, as well as other components and elements of the instrument.

The sampling inlet has been designed to provide easy flow access into the inlet duct, while at the same time protecting the interior of the HCDM from the entry of rocks, and other debris, by means of a horizontal plate which creates a radially symmetrical inlet flow. As mentioned before, this type of inlet is the preferred configuration for a number of recently developed particulate sampling devices designed to minimize particle discrimination resulting from free air speed and direction effects. It is expected that, within the mine environment, the prevailing ventilation flow patterns will be in the horizontal plane, which is the preferred one for the selected inlet geometry. Other applications for the HCDM may require the use of an inlet designed for isokinetic sampling. A 45° conical section follows the annular inlet in order to provide a gradual transition to the vertical flow duct leading into the beta sensing area. The upper 7.5 cm of that 1.5 cm diameter duct is of circular cross-section, which is followed by an oblong cross-section whose parallel sides contain the beta radiation source and the detector. A divergent transition section precedes the expansion into this oblong cross-section. The two sensing elements are slightly recessed back from the duct such that the clean air curtain is allowed to flow over the two sensitive surfaces. Following the detection region, the duct expands into the filter-cartridge holder as shown in Figure 2.

The inlet duct, sensing chamber and filter section were designed to emphasize minimum obstruction to the dust laden flow and to ensure the development and maintenance of a laminar flow regime required both to minimize wall deposition of particles, as well as to ensure the integrity and laminarity of the clean-air flow curtain over the source and detector primary surfaces.

The source disc is held in position by a threaded plug with a screwdriver slot. Removal of the source would be necessary only if its surface becomes soiled with dust. The detector can also be removed if required (either because it has become soiled or because of internal failure). Diagnostic indications (to be discussed further on in this report) on the instrument display are provided to determine whether cleaning is required, or if the detector must be replaced.

As indicated previously, the inlet section can be removed from the rest of the flow assembly by loosening three thumb-screws (see Figure 2).

Flow Subsystem

The functions of the flow subsystem of the HCDM are to: (a) sample and introduce air from the surrounding environment into the sensing region of the instrument, (b) provide a clean-air curtain over the beta source and detector, and (c) to supply a clean-air purging flow during the zero reference periods.

The use of a solenoid valve to effect flow switching during the zero check operation was rejected because these valves consume an appreciable amount of power during their activated condition and generate a significant pressure drop, both properties being incompatible with battery operation and practical weight restrictions. Consequently, and after careful review and evaluation of commercially available devices of this type, it was decided to design a valve specially compatible with the needs of this project. The specific requirements for this device were (a) three way, (b) low power d.c., (c) negligible pressure drop in the open direction (d) compact and low weight, and (e) reliable under shock, vibration, high humidity, etc.

A prototype valve was designed, fabricated and tested. The results indicated that it fulfilled all of the preceding conditions. The operation of this valve is based on the same principle as that of the so-called peristaltic pumps; i.e., lateral compression of a flexible piece of tubing. In the present design either one or the other of two such pieces is compressed by an eccentric motor-driven cam, as shown in Figure 12. Two micro-switches serve to stop the motor for 180° rotation of the shaft at the angular position required to seal either one or the other duct. Dynamic braking, by shorting the motor leads, is used to prevent rotation overshoot. A miniaturized version of that prototype has been designed and incorporated within the HCDM.

Figure 13 depicts the flow configuration of the HCDM. Normally, i.e., during the dust sensing operation cycle, flow enters through the sensing chamber, then through the high capacity filter where all dust is retained, through the backup filter cartridge, through the pump (which runs continuously), through the 3-way valve (bottom branch in Figure 13), and finally out through a small flow resistance element. A small fraction of the filtered airflow is diverted to provide the clean-air curtain flow provided to prevent dust deposition on the beta source and detector surfaces. A high flow resistance element ensures proper distribution of this small secondary flow.

During the purging period of the operating cycle (i.e., to establish zero dust concentration conditions within the sensing region) the 3-way valve is switched to its opposite position, closing the exhaust branch and feeding the entire pump flow through the clean air purge line (see Figure 13), thus purging the sensing chamber for zero reference determination.

A high capacity filter cartridge for in-line operation, manufactured by MSA (part 95302, type H), is used on the HCDM. It operates with a clean-filter pressure drop of only 0.06 in. H_2O at a 2 l/min flow rate.

Pulsation dampeners are incorporated on both the inlet as well as exhaust sides of the diaphragm pump in order to reduce flow pulsations to a low enough amplitude. The mounting positions of the principal flow subsystem components are shown in Figure 2. The flow subsystem operation is based on sensing the pressure drop across the exhaust flow restrictor (see Figure 13) by means of an adjustable pressure switch whose condition (i.e., either open or closed) controls the operation of the electronic drive circuit of the pump motor. This signal is sensed by the microprocessor CPU which controls a switching voltage regulator to regulate the pump speed. The switching regulator utilizes the pump motor inductance to decrease current consumption.

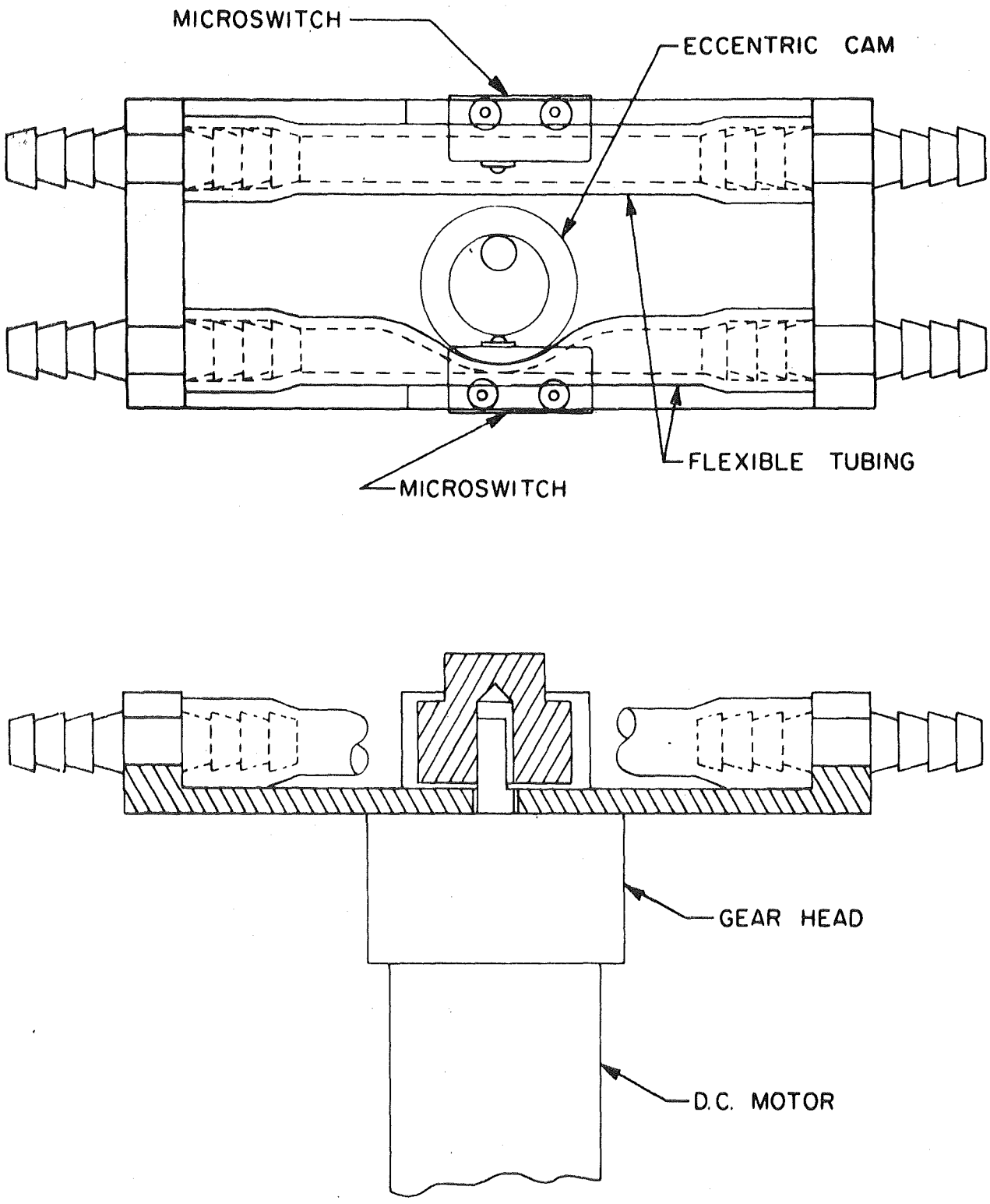


FIGURE 12. - Three-way flow valve developed for HCDM.

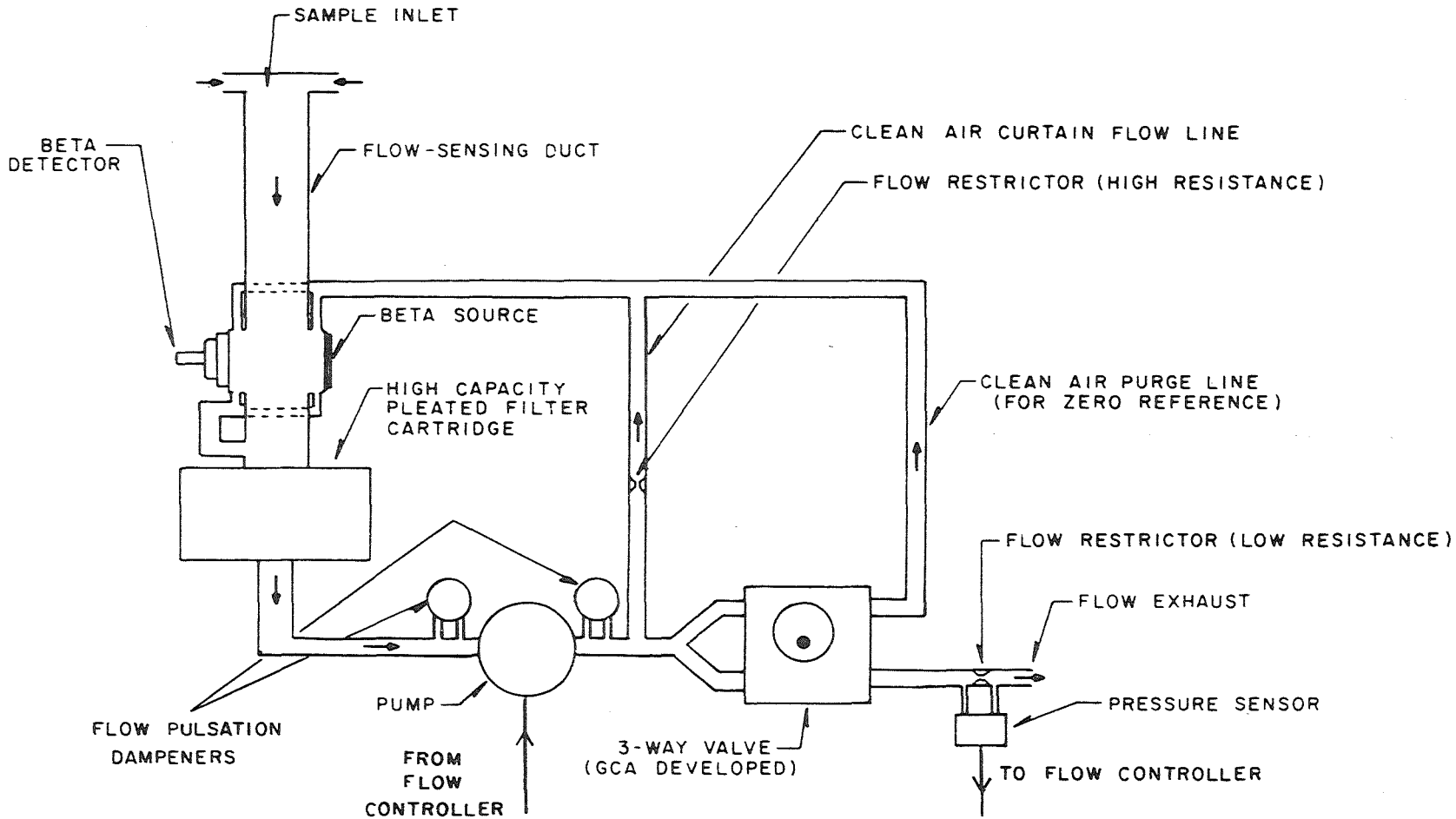


FIGURE 13. - Flow system of HCDM.

In theory, the flow would slowly hunt around the hysteresis pressure of the pressure switch. In practice, however, the average flow remains constant due to the pressure switch opening and closing for every pump pulsation. The downstream pulsation dampener is added to minimize this pulsation and help maximize the life of the pressure switch. A Micro Pneumatics Logic 3" H_2O pressure switch is used for this application. The switch contact current is very low, which adds to the lifetime, and the circuit is relatively immune to contact resistances of less than 10 kilohms.

A flow rate of 2 l/min $\pm$ 3 percent can thus be maintained over the range of 2 to 50" H_2O pressure drop upstream of the pump.

The pump selected for this application is a high reliability single diaphragm pump manufactured by Delta Power (Model PV-1100) of Medway, Mass. It incorporates an advanced, high quality d.c. motor (manufactured in Switzerland by Portescap), with an ironless rotor. It operates at very low (and thus intrinsically safer) voltages of the order of 3 to 5 volts. This same type of motor is used for the 3-way valve described previously in this report. If the pressure drop across the filter cartridge exceeds about 50 inches H_2O, the flow controller-pump combination can no longer maintain a constant flow rate and an alarm indication is displayed suggesting that the filter cartidge should be replaced.

During the purging cycle, the pump is not under feedback control and is powered up (by the microprocessor) to run at maximum speed in order to accelerate the dust clearing operation.

Electronic Subsystem

General Description

The electronic circuitry of the HCDM has been designed around an eight bit microprocessor of the CMOS family of semiconductor large-scale integrated circuits. This general type of circuit provides the required flexibility, stability and low power consumption for this type of portable battery operated monitoring instrumentation. The storage of updated reference information (i.e., the zero-concentration beta counts, over periods of several minutes to possibly tens of minutes); the accurate computation of the mass concentration; the precise control sequencing to alternate the operation of the purge valve with the required waiting intervals of a few seconds for the transient flow settling times; diagnostic indications of abnormal beta count rates and excessive filter pressure drops; data recording and averaging; and data count rates and excessive filter pressure drops; data recording and averaging; and data playback in various selectable formats, etc., are all functions that this microprocessor-based circuitry performs within a very small volume and with an exceedingly low power consumption.

The microprocessor program, accessed and controlled by the front panel touch switch array, provides the user with enormous operational versatility; a vast variety of measurement, display, averaging, and data playback combinations can be selected, satisfying essentially any foreseeable requirement.

Figure 14 depicts the block diagram of the microprocessor-based circuitry of the HCDM. It is centered around the RCA CDP1802 microprocessor, and uses several other CMOS peripheral components.

Power consumption during instrument operation is estimated to be about 300 mA at 6V, without display activation, and about 400 mA at 5V with display activation during the purging cycle. The 6-volt gelled-cel type rechargeable battery used on the HCDM has a nominal capacity of 6 ampere-hours, with which the instrument can be operated for a minimum of 12 hours between recharging cycles.

The microprocessor normally lies dormant with negligible battery loss in a memory retention mode to store constants and previously measured values. When the RESET switch is pushed, the microprocessor circuit power is completely restored and a decimal point will be displayed. If no other key is depressed within 30 seconds then the power is again shut off. If the MEAS key is depressed, the measurement cycle is entered. The beta detector high voltage power supply is first turned on for warm up, and the clean-air purge flow is turned on to high speed for 5 seconds to rapidly purge the sensing duct. The pump is then switched to the normal speed to provide a positive pressure clean-air supply to the sensing head flushing out all dust while the reference beta count is taken. This beta count is then checked to ensure that the G-M tube is not faulty. This count can be displayed for diagnostic checking. The battery voltage is then checked in order to determine whether it was sufficient to perform the beta count. This first reference beta count is then checked with previous clean air beta counts.

The 3-way valve is then cycled to the normal sampling position. The pump is first operated at a higher than normal speed for more rapid sample concentration attainment. After a few seconds (in order to reach dust concentration equilibrium) the pump speed is decreased to normal and a 10-second beta count is taken.

The mass concentration for each 10-second dust measurement is computed from the updated reference beta count and from each 10-second beta count during the sampling period. During these 10-second periods, the microprocessor performs three functions. It counts the beta pulses, regulates the airflow, and checks whether the 10 seconds have expired. After 10 seconds a mass concentration calculation*(7) is performed and averaged over the

---

*Conc. = K (log upcount - log downcount), where log function is computed from:

$$\log_2 X = C_1\left(\frac{X-1}{X+1}\right) + C_3\left(\frac{X-1}{X+1}\right)^3 \qquad \frac{1}{\sqrt{2}} < X < \sqrt{2}$$

$$-5 \times 10^{-6} < \text{error} < 5 \times 10^{-6}$$

---

selected sampling period. The total mass concentration range of the HCDM is 0 to 500 g/m^3; zero, as well as negative values (resulting from statistical

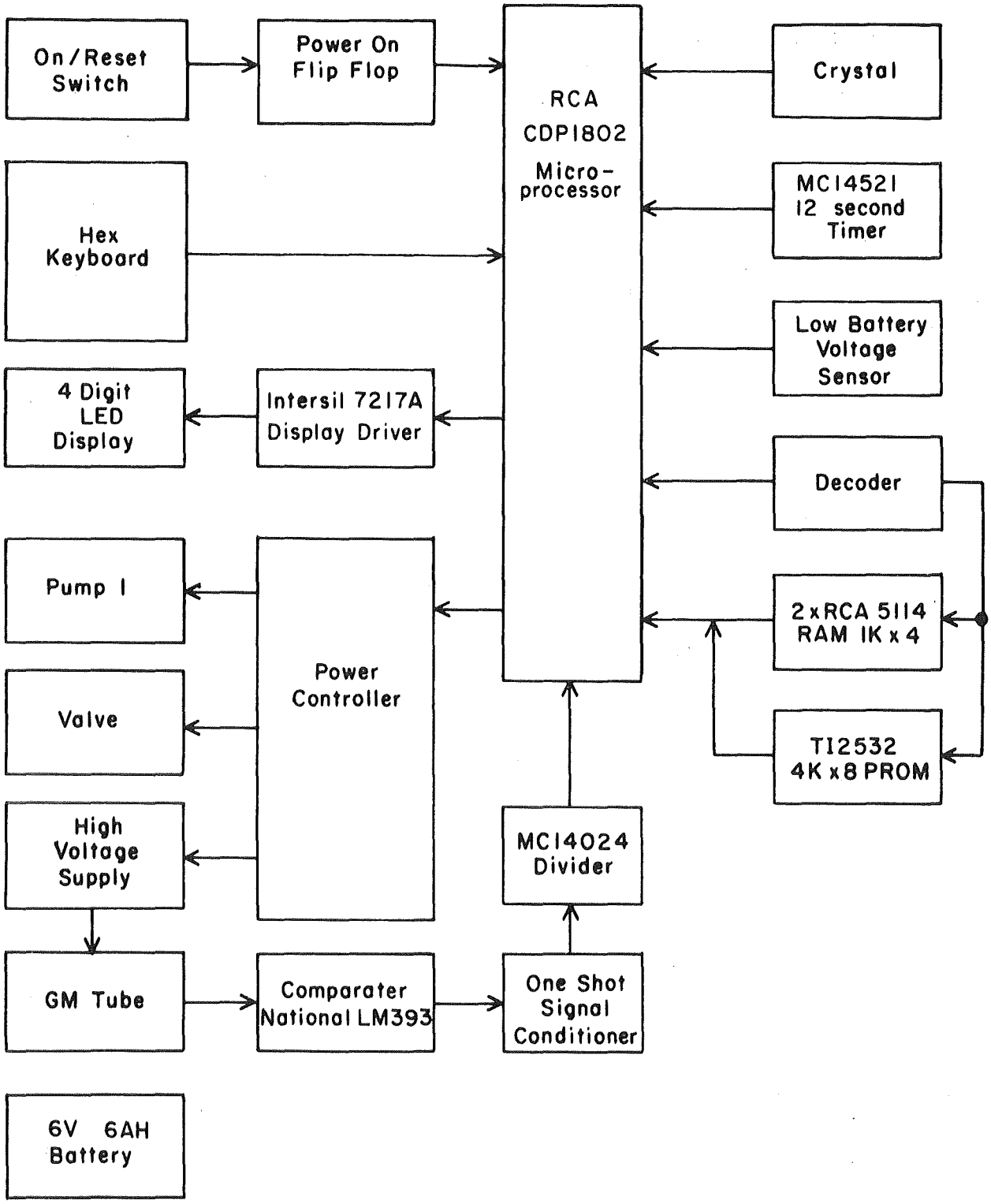


FIGURE 14. - Block diagram of electronic circuitry of the high concentration dust mass monitor.

beta count fluctuations at or near zero concentration levels) are displayed as a single dot. The 10-second average can be displayed continuously, or for 2 seconds to conserve battery power, or the selected time average can be displayed. The average can also be transmitted via a digital ASKII 20 mA current loop, a 0-20 mA analog loop, or a 4-20 mA analog loop. If the concentration exceeds a preselected limit, a 20 mA alarm signal can be transmitted.

A new 10-second measurement period will then be initiated unless one of the following conditions exists:

a) The preselected total run time is exceeded

b) 960 sampling periods are exceeded

c) The battery voltage drops to an unacceptable level (i.e., 5.2V)

d) A new purge cycle is required (e.g., once every 3 minutes)

e) RESET has been commanded

The HCDM may be stored for many months before playing back the data contained in its memory. The data playback may be via its own display, a digital printer (20 mA ASKII), 0-20 mA analog, or 4-20 mA analog. When the data is no longer required it may be erased by pushing the RESET and CANCEL controls at the same time. All the operator then need do is to charge the unit, place it in location, push RESET then MEAS and leave it to complete its next sampling run.

A separate Instruction Manual has been provided containing a detailed description of the measurement, playback, and change of constants operations procedures as well as default and error code displays.

The Geiger detector is operated from a high voltage power supply with a feedback regulation circuit. The +950 volt output varies by less than $\pm$ 2 volts over the input battery voltage range of 5 to 7.5 volts. Tight regulation is required to ensure beta counting stability and repeatability.

The D/A converter circuit uses a novel op amp current amplifier circuit which requires only a single positive power supply. It exhibits a 1 percent change in output current over the supply voltage range of 5 to 7.5 V DC.

The software flow chart diagrams of the HCDM are presented in Figures 15 through 25. The power up routine diagram shows the logic upon pressing the RESET switch and how the various modes of CHANGE CONSTANT, MEASURE, and PLAYBACK are entered. The check default values subroutine initializes the system constants if they have never been previously set. The change constant subroutine shows how the constants are modified from the front panel keyboard, and depicts the binary coded decimal conversion subroutine to convert decimal keyboard entry to binary. The measurement subroutine shows most of the logic

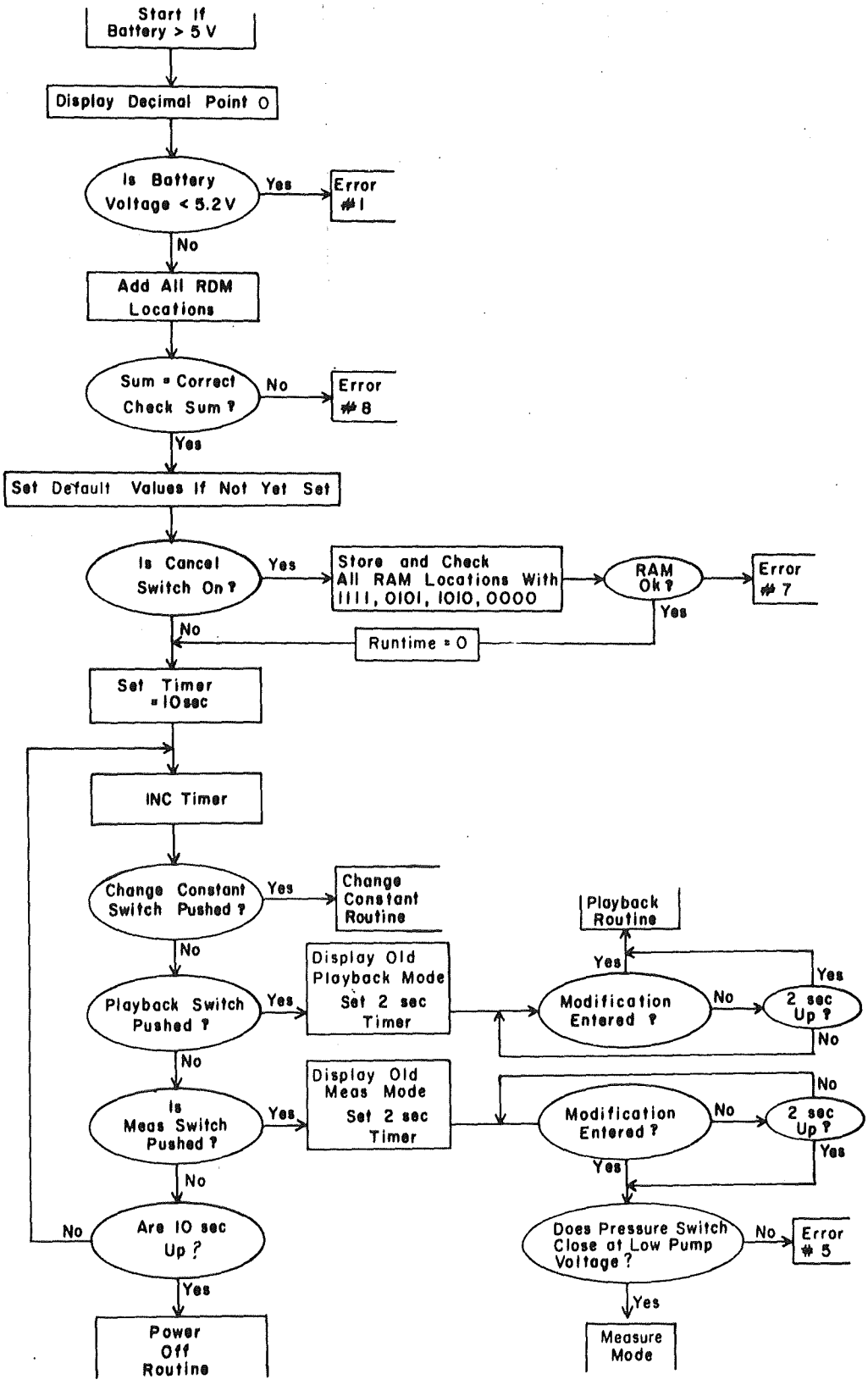


FIGURE 15. - Start routine logic flow diagram. (entered when RESET is pushed).

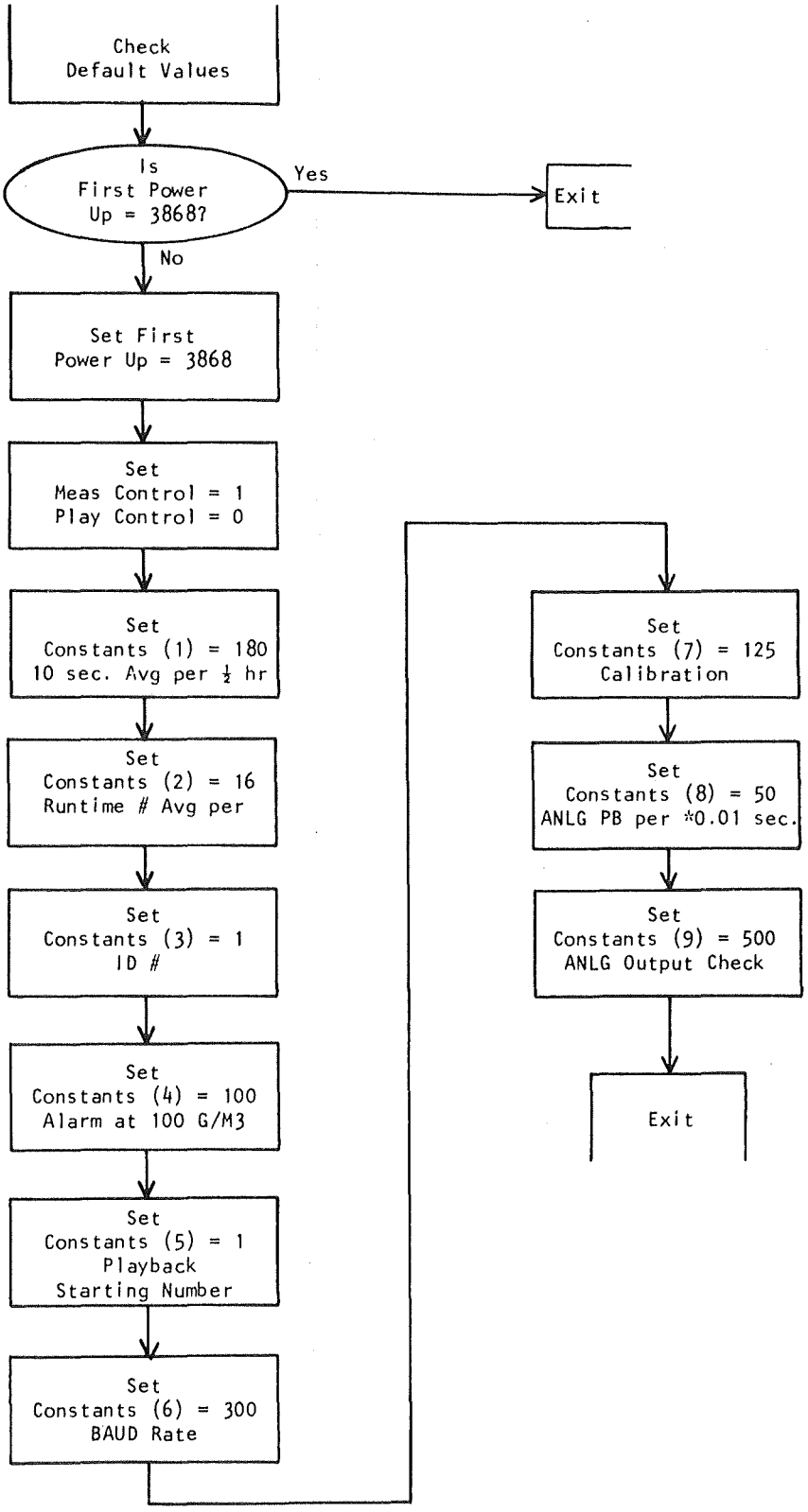


FIGURE 16. - Check default value logic flow diagram.

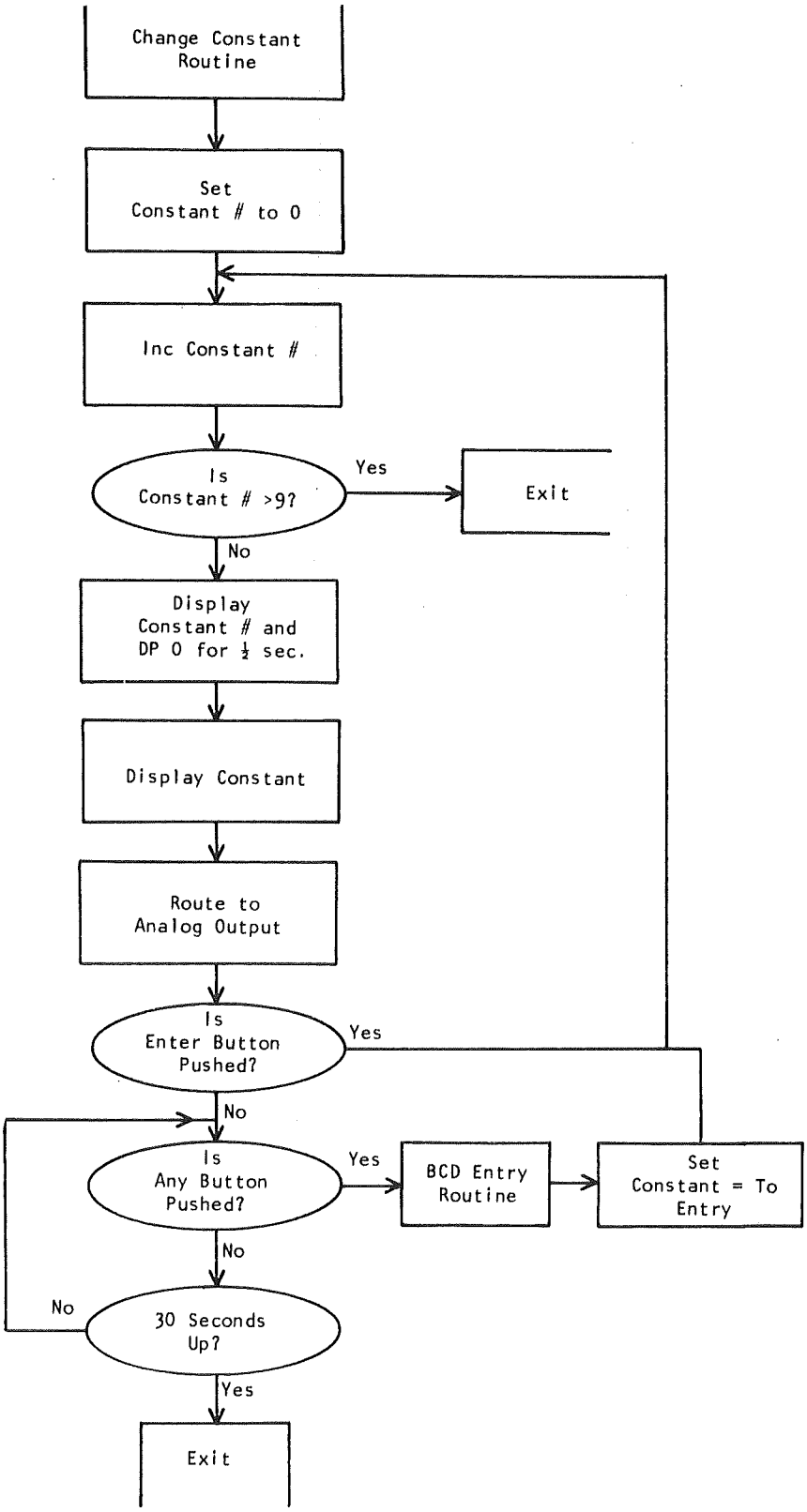


FIGURE 17. - Change constant routine logic flow diagram.

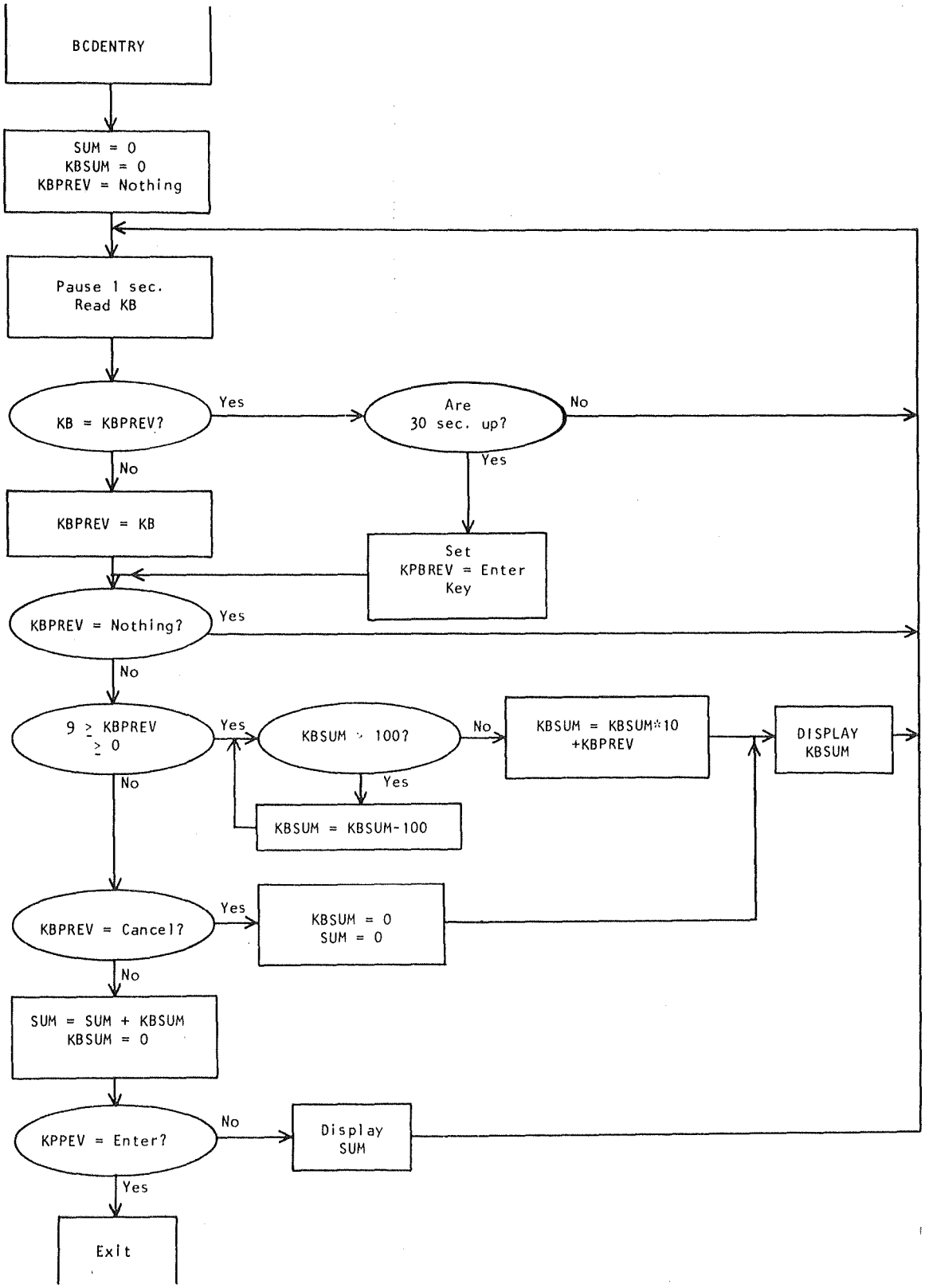


FIGURE 18. - BDC entry routine logic flow diagram.

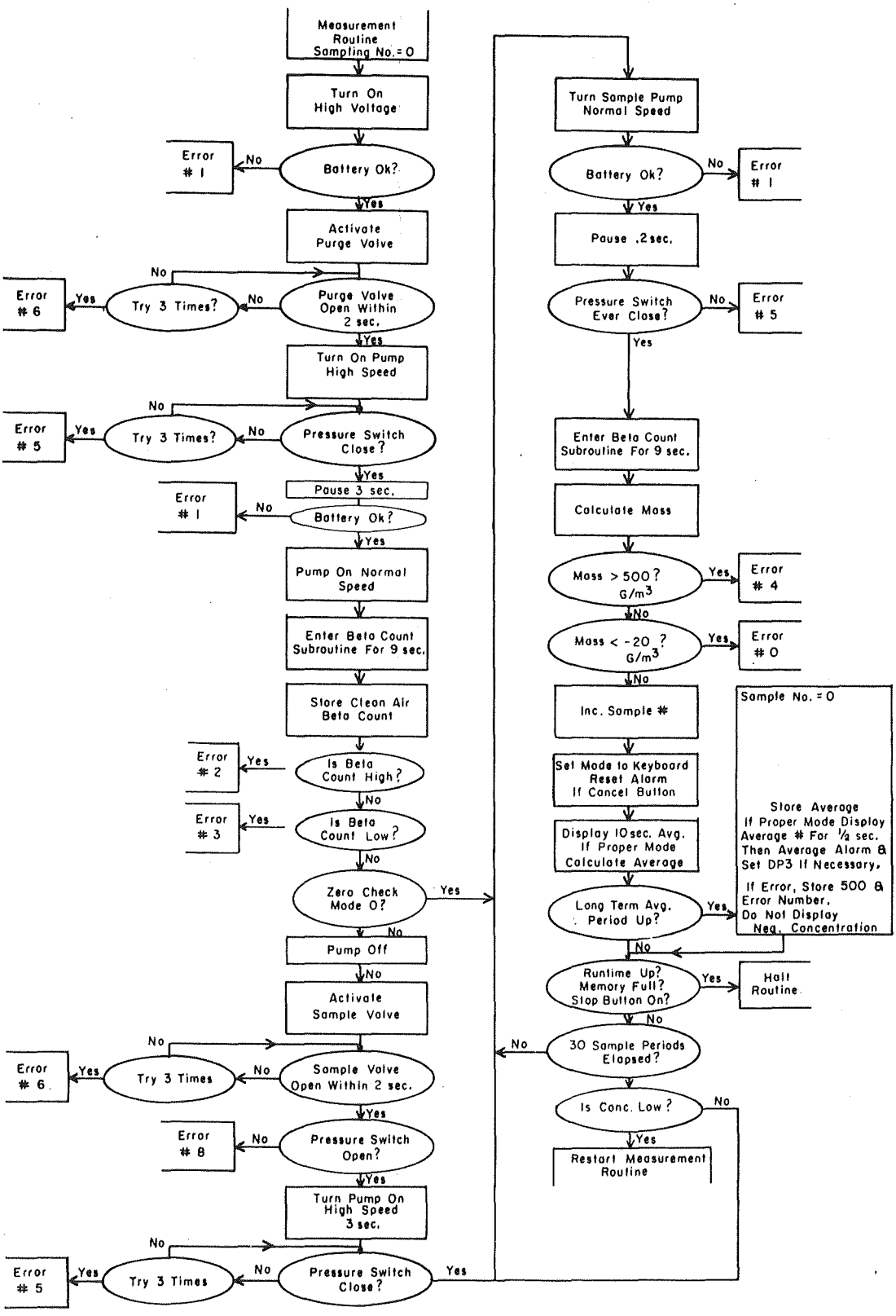


FIGURE 19. - Measurement routine logic flow diagram.

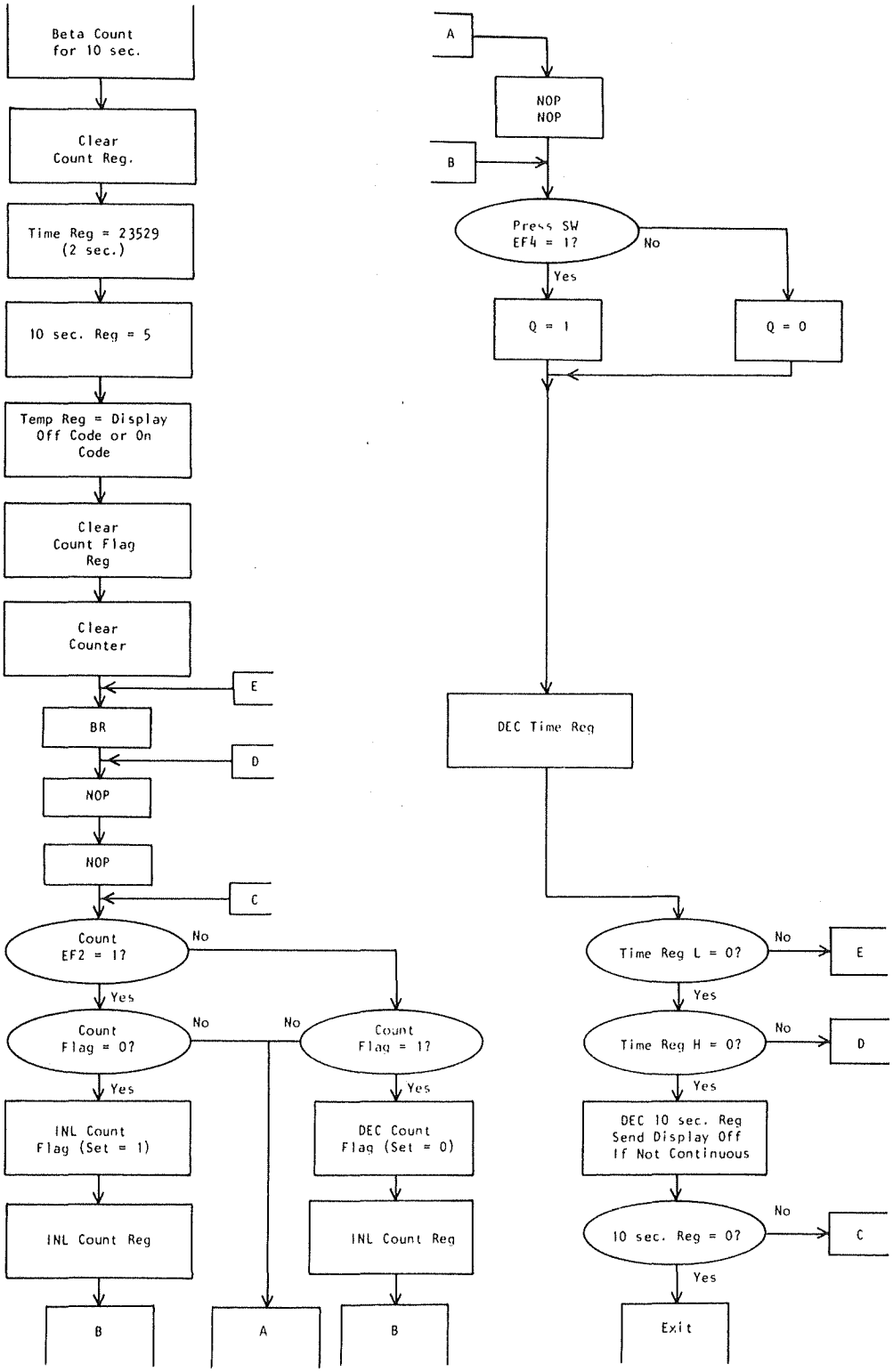


FIGURE 20. - Beta count routine logic flow diagram.

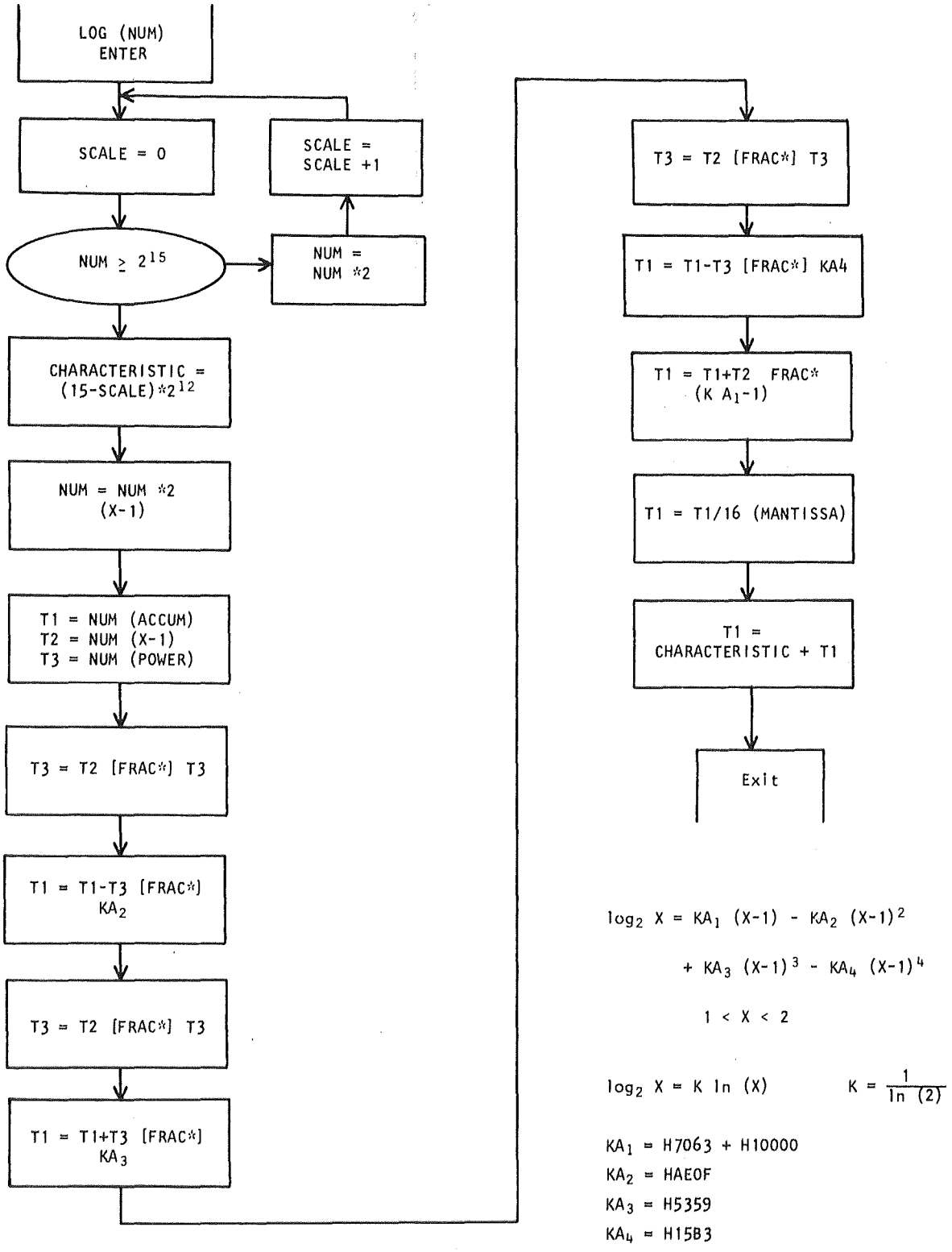


FIGURE 21. - Log routine logic flow diagram.

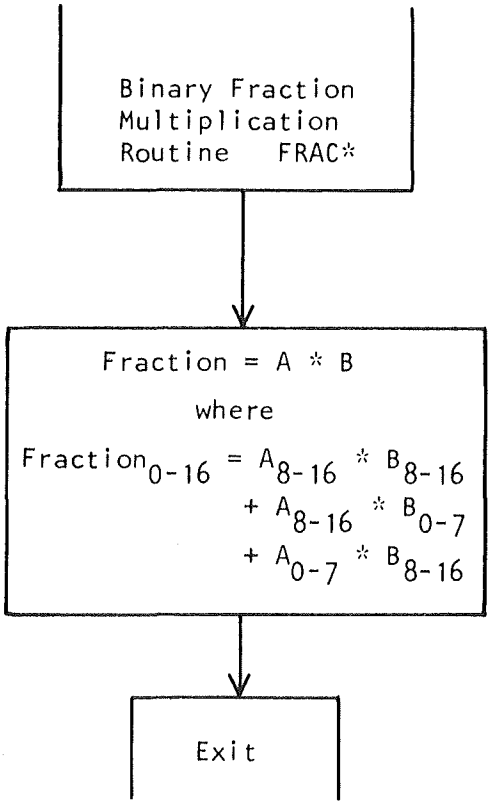


FIGURE 22. - Binary fraction routine logic flow diagram.

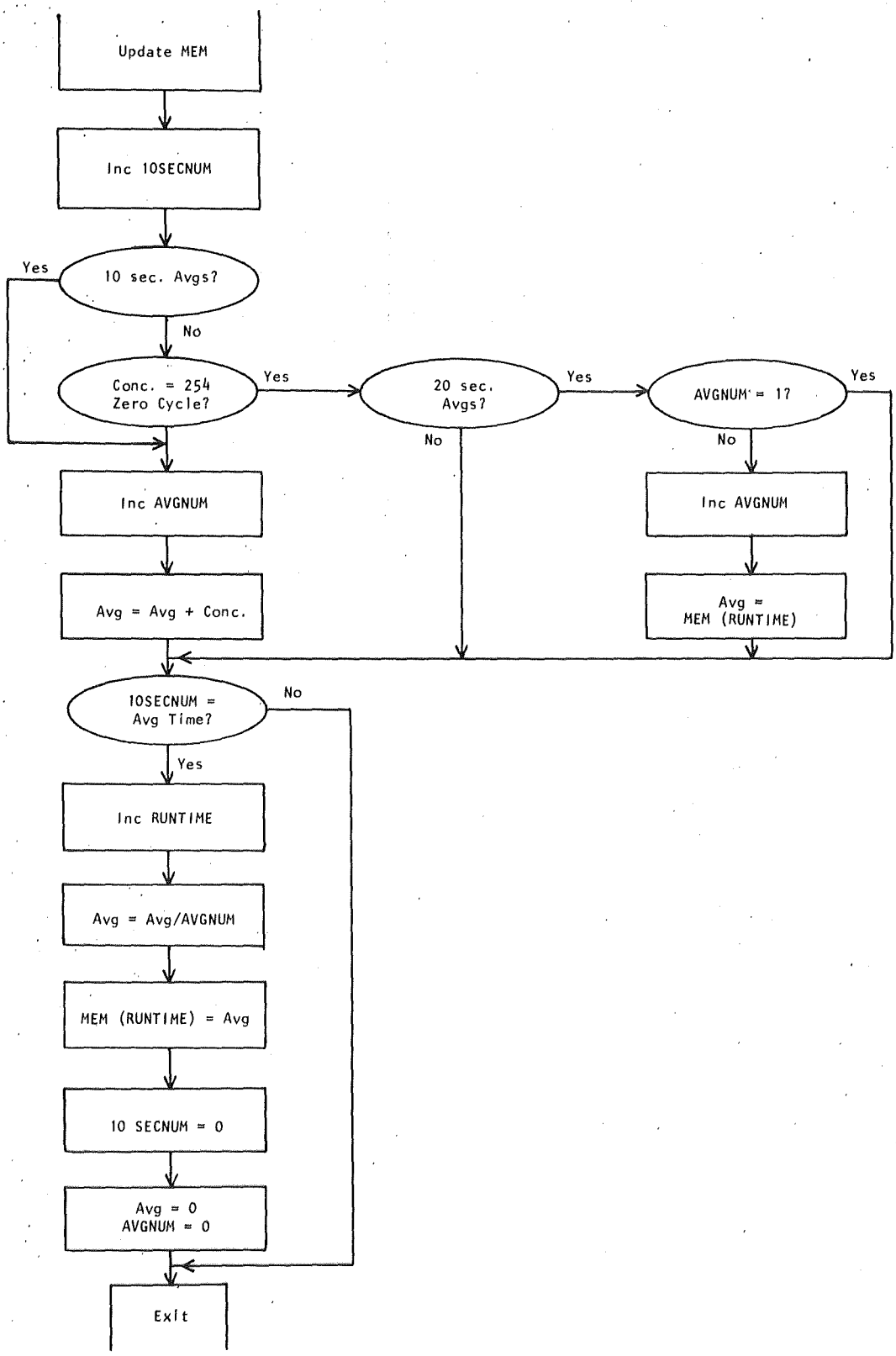


FIGURE 23. - Update memory routine logic flow diagram.

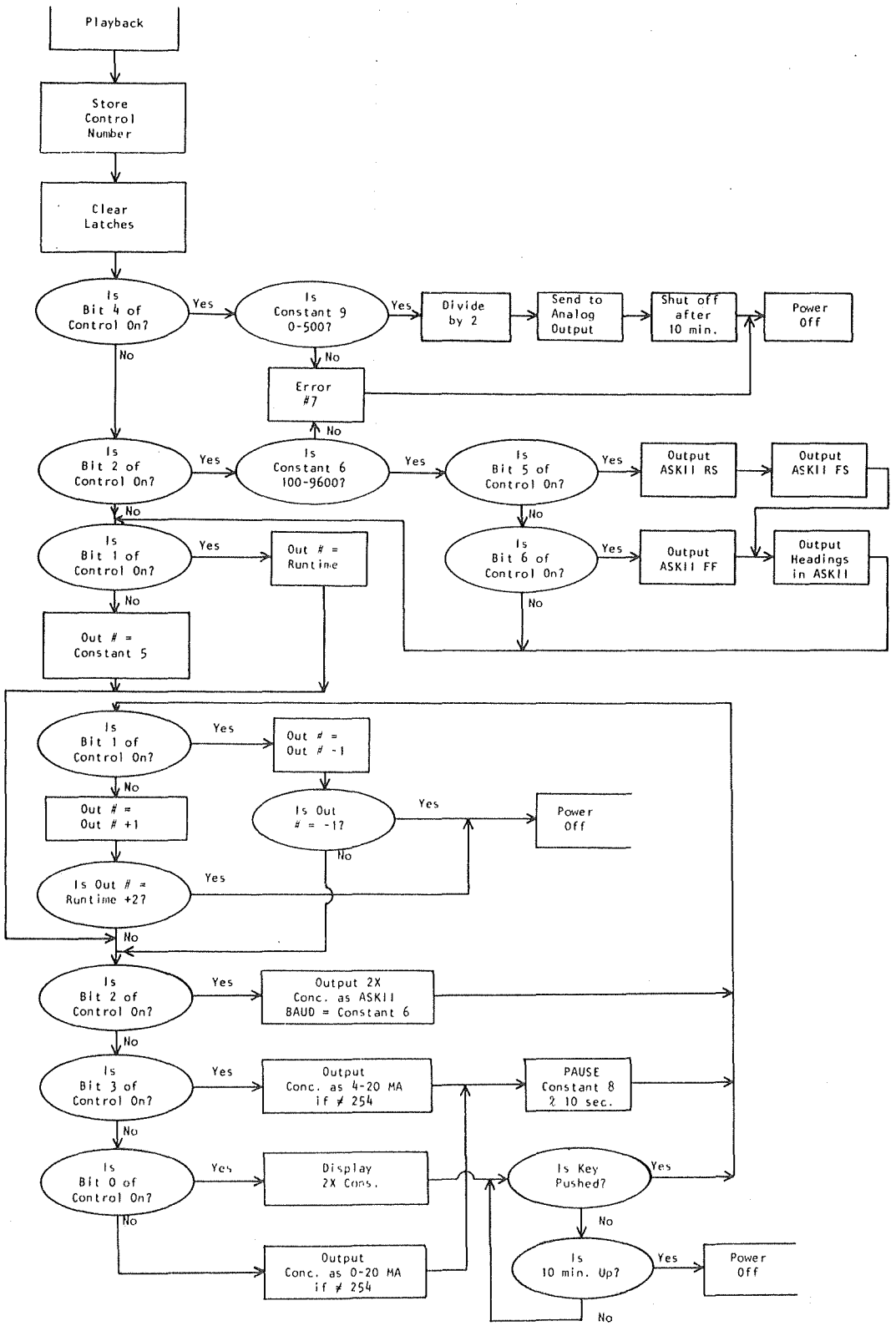


FIGURE 24. - Playback routine logic flow diagram.

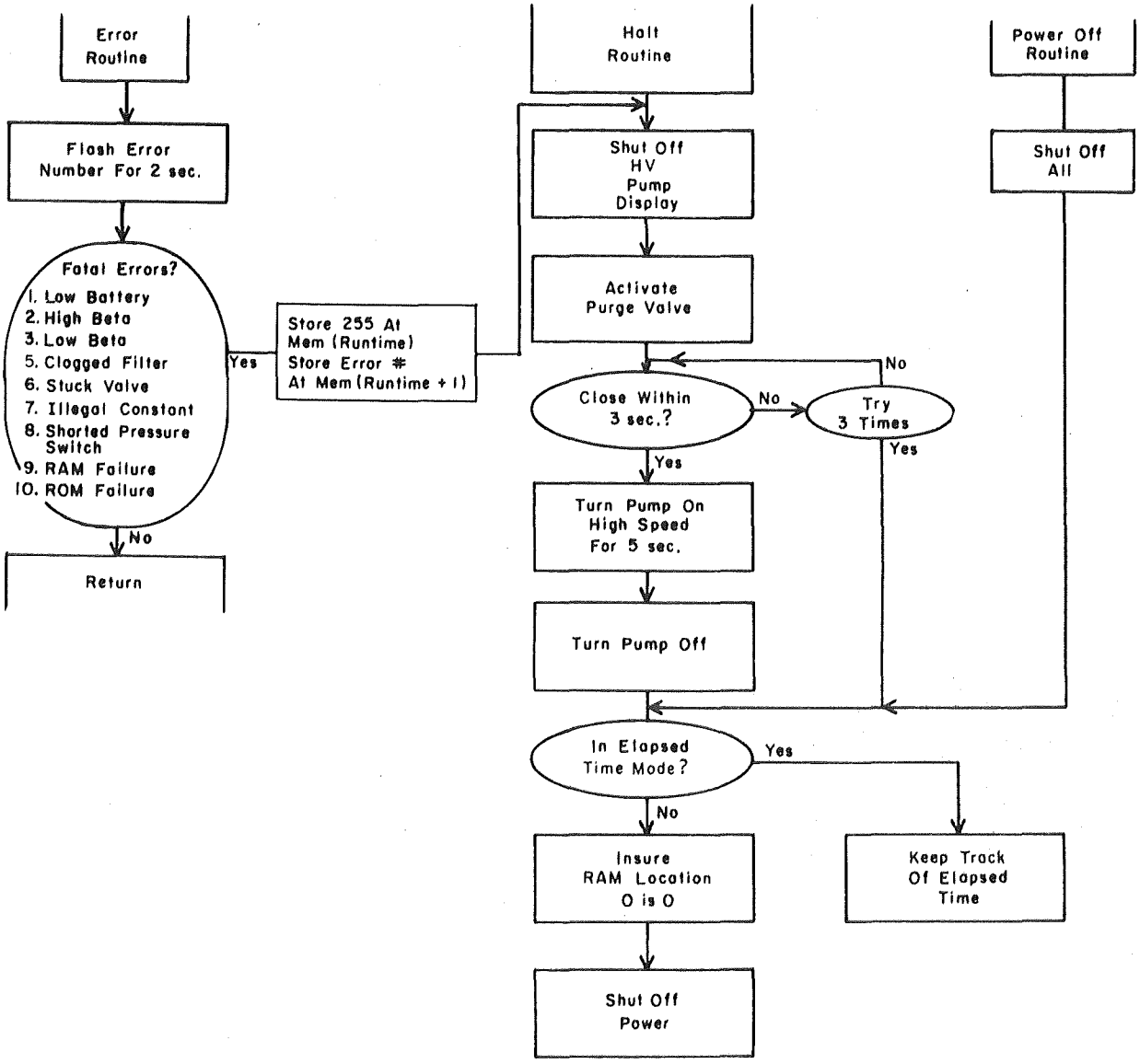


FIGURE 25. - Error routine logic flow diagram.

during the MEASURE mode as well as the beta count subroutine, the log subroutine, the binary fraction multiplication subroutine, and the update memory subroutine. The playback subroutine shows the logic during the PLAYBACK cycle. The last flowchart shows the error, halt, and power off subroutines.

During the electronic design/development effort, the following changes were implemented to the originally configured system:

a) The RAM memory was expanded from 1024 x8 to 3072 x8 in order to accommodate the 2880 bytes of storage needed for 8 hours of consecutive 10 second averages.

b) The purge cycle was restructured as follows:

	Action	Seconds	Elapsed Time Seconds
1.	Rotate purge valve	2	2
2.	Pump at full speed	3	5
3.	Conduct beta count	10	15
4.	Rotate sample valve	2	17
5.	Pump at full speed	3	20

c) When using the analog output with 10 or 20 second average periods, the measured concentration during the period just prior to the purge cycle remains at the output during the purge cycle period. The alternative would have been to display a zero or full scale indication which could confuse the interpretation of a strip chart recording. During digital playback, however, the value 508 is displayed to signify a zero cycle.
The schematic diagrams of the HCDM electronic circuitry are shown in Figures 26 and 27. All the circuit elements are contained on a single 9.5 by 7.5 inch printed circuit board. The development of the circuitry was performed using a wire-wrap version which was used as a breadboard.

d) The potential problem of dust access to the sensing volume during a zero-concentration or purge cycle, due to particles entering by convection or sedimentation was considered. It was decided that implementation of an adaptive zero check routine would provide a practical solution to this problem. This approach consists of a software modification wherein the purge cycle to establish the zero reference beta count is performed only if a number of preceding dust measurements indicated that the dust level was below a set maximum, e.g., 20 g/m^3, thus minimizing the probability that passive dust contamination, associated with very high concentrations, could affect the reference measurement.

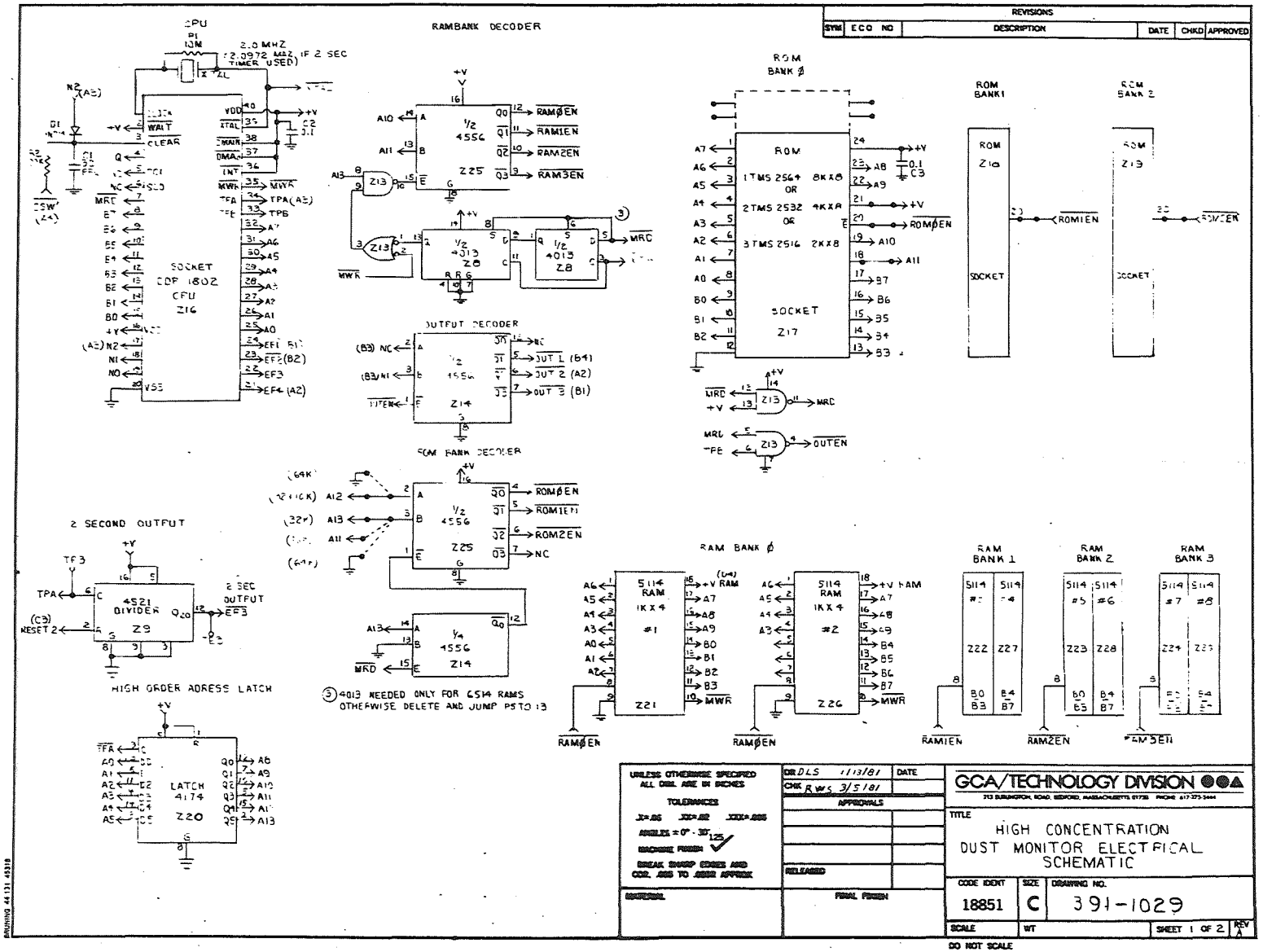


FIGURE 26. - Schematic diagram.

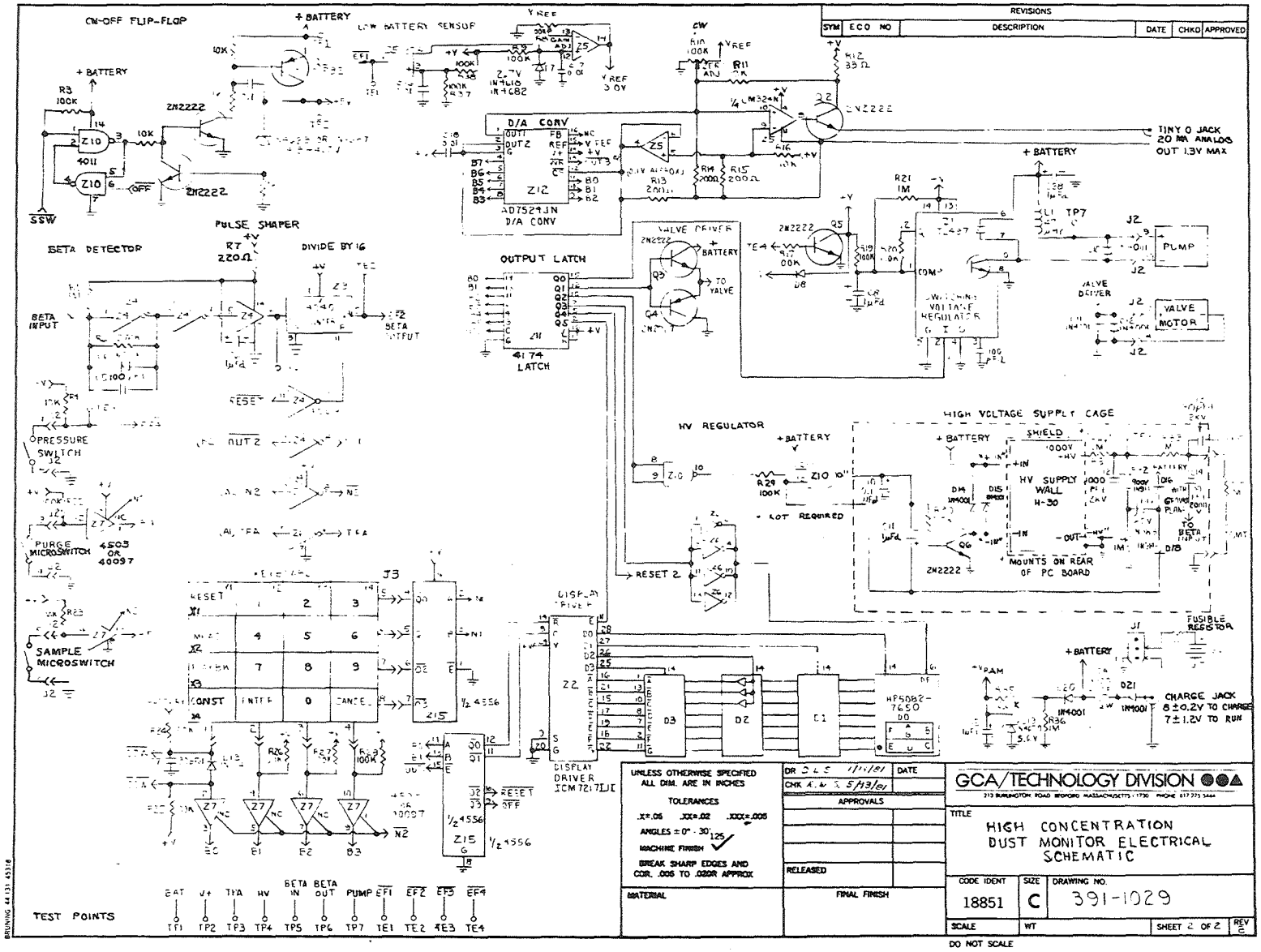


FIGURE 27. - Schematic diagram.

Panel Controls

The front panel, whose layout is shown in Figure 28, contains an LED display with a battery charge jack, a data out jack, and a keyboard:

- LED Display--Four 0.43 in. tall high efficiency LED characters.
- Charge Jack--A jack with a spring loaded dust cover for charging the battery. Contains internal series diode so that a short circuit cannot cause any spark hazard.
- Data Out Jack--A two-conductor jack for driving either:
    (1) An analog recorder (0-20 mA output)
    (2) An analog telemetry line (4-20 mA output)
    (3) A digital printer (20 mA loop)
    (4) An alarm indicator (20 mA max.). The alarm level can change only during the measurement mode. In playback mode the jack contains data output information.
- Keyboard--A flush mounted touch keyboard of approximately 4 x 4 in. total area with 16 keys. Switches are sealed and when touched, the key is shown on the LED display.

Error Codes

If an error exists, the LED Display will flash an error code number for 10 seconds. The HCDM will then shut off automatically if a "maintenance" (M) error has occurred. The codes are:

0) Concentration <-20 g/m^3

1) Low battery voltage (M)

2) Too high a beta count. Tube may be defective. (M)

3) Too low a beta count. Tube may be defective. (M)

4) Concentration >500 g/m^3

5) Change filter (M)

6) Purge valve stuck (M)

7) Illegal constant (M)

8) Shorted pressure switch (M)

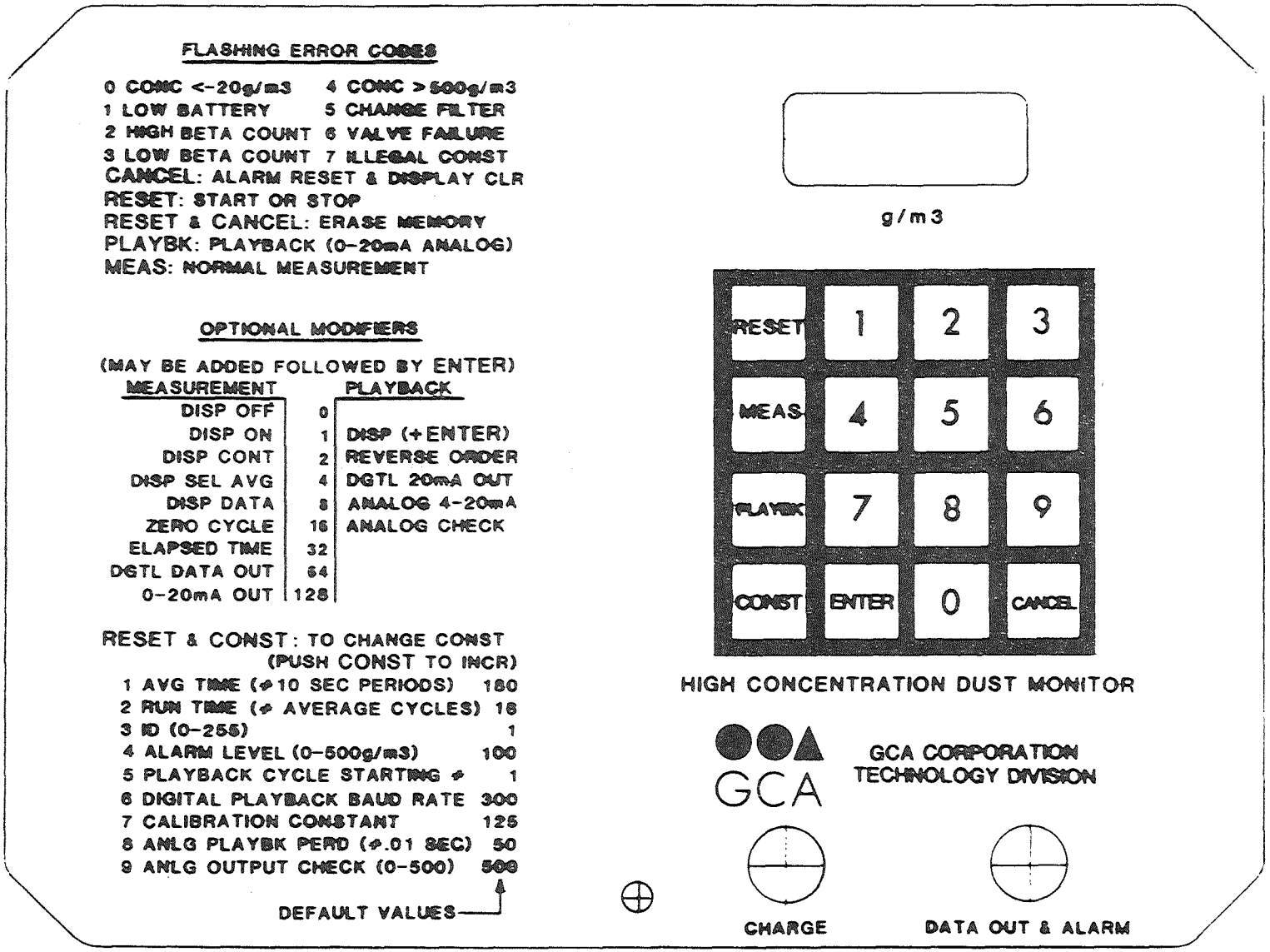


FIGURE 28. - Layout of front panel of HCDM.

9) RAM Failure (M)

10) ROM Failure (M)

Intrinsic Safety and Radioactive Source Licensing Aspects

1) Battery and Charge Circuit--The battery assembly has an internal fusible flameproof current-limiting resistor potted into the battery. The battery charge jack and battery are in series with a 1N4001 1A diode so that current can only flow into and not out of the charge jack.

2) High Voltage Power Supply--The HV supply is a Wall Industries H-30 supply. Feedback from the output is used to regulate the input current to produce 950 V on the output. The output voltage is proportional to the input voltage. If the input regulator should fail, the maximum voltage which could be applied would be the battery voltage. The supply is rated 1KV to 3KV output for 4 to 12 VDC input. A fully charged battery delivering 7.5 VDC would cause an output of 1.9 KV thus the output capacitors are rated at 2 KV. The high voltage power supply is rated at 1 mA maximum output current.

   The HV supply connects to a series 1 MΩ resistor followed by a 1000 pF filter capacitor. Another 1 MΩ series resistor separates the GM tube from this point.

   Two 1N4001 reverse biased diodes are across the HV supply driver transistor to protect the transistor when switching off the HV supply inductive load. The HV components external to the power supply are potted.

3) The ESCAP 3-way valve motor has two 1N4001 reverse biased diodes across its input to protect the driving transistors from switching off an inductive load.

4) The ESCAP pump motor is in series with a 47 μH coil to increase its total inductance. a TL497A switching voltage regulator uses this inductance to limit the current to the pump rather than wasting it across a series pass transistor.

   The control feedback loop is as follows. If the pressure switch senses no pressure the microprocessor (μP) turns on the 2N222 driver transistor thus enabling the TL497A. The μP also turns on its Q output line. Since this is in series with a low pass filter, the control voltage to the TL497 slowly rises. The TL497 sends full duty cycle pulses to the pump until the pump voltage, smoothed by the pump and 47 μH inductance, reaches the control voltage.

The μP will continue to increase the pump speed until the pressure switch closes due to normal flow conditions causing the correct pressure to occur across the series orifice. When this occurs, the microprocessor turns off its

pump drive Q line (see Figures 26 and 27) until the pressure switch turns off and the cycle is repeated. During a purge cycle, the microprocessor Q line is always on to produce maximum pump speed.

There is a 1N4001 reverse biased diode across the pump, a reverse biased diode internal to the TL 497, and a 1N4001 reverse biased diode across the 2N2222 driving transistor (refer to schematic diagram of Figures 27 and 28).

All other electrical elements are either of the very low power consumption type, i.e., CMOS semiconductors, or are already approved for intrinsic safety on other instruments. As mentioned above, standard circuit design practices such as diode protection across the pump terminals and other critical elements have been implemented to adhere to intrinsic safety guidelines, as well as to prevent current reversal through the charging connector.

The use of digital circuitry throughout provides greatly enhanced imperviousness against high humidity-related problems by eliminating the typical susceptibility to spurious high impedance leakage paths exhibited by analog circuitry.

As far as the radioactive Ni-63 beta source is concerned, GCA/Technology Division has a general license from the NRC under Title 10, Part 32, Section 32.26 of the Code of Federal Regulation which exempts users from requiring a license for the employment of instruments containing a radioactive source that are "gas and aerosol detectors." This regulation requires that GCA request a routine amendment of its general license for every new type of instrument falling within this category. Such an amendment has been granted for the Ni-63 Source contained in the HCDM, such that the eventual users of this instrument do not require any licensing whatsoever, even if the activity of this source exceeds the exempt activity maximum stipulated in Title 10, Part 30, Section 30.71, Schedule B of the Code of Federal Regulations.

Instrument Packaging and Layout

The overall design of the HCDM prototype was guided by the following specific objectives and criteria:

- Maximum ruggedness to enable it to withstand the most extreme conditions of impact, vibration, abrasion, etc.
- Portability by a single person
- Ease of deployment, mounting or suspension
- Easy access to interior of the instrument for maintenance and/or repair
- Ease of field replacement of filter cartridge, without requiring access to interior of the instrument

- Rugged, nonprotruding and protected controls and readout
- Clear, large, self-illuminated readout display
- Ease of replacement of battery
- Compatibility with and adherence to intrinsic safety requirements

The housing of the HCDM consists of a 1/4-inch thick cast aluminum box whose outside dimensions (in inches) are shown in Figure 2.

All internal components are mounted to a plate which, in turn, is mounted to the front panel by rectangular standoffs. In order to gain access to the interior of the HCDM, only knurled thumbscrews need to be loosened. The procedure is as follows: (a) remove sample inlet flow duct, (b) remove bottom support of filter cartridge holder, and (c) pull out front panel assembly.

The battery, a rechargeable sealed gelled-cell type, is held in position by means of a high-strength expandable strap, and can be removed easily, if necessary. This battery, its mounting, and the integral intrinsic safety fusible resistor are identical to the configuration used on the portable light scattering dust monitor (GCA Model RAM-1) originally developed for the Bureau of Mines.

The high capacity filter cartridge can be replaced in a few seconds. Referring to Figure 2, loosening one knurled screw frees a swing-away bar which, in turn, allows the removal of the bottom filter compartment cover and the filter cartridge.

Two-side handles are provided to carry the HCDM, and four eye bolts are attached to the top surface of the enclosure in order to provide solid attachment points from which the monitor can be suspended, if so desired.

The front panel sealed touch-switch control array and the LED display are protected by a hinged transparent acrylic cover, recessed into the panel. Both the battery charging connector and the data playback-recording connector are accessible through the protective cover after lifting a spring-loaded cap. Both connectors are directly accessible when lifting the front cover.

Calibration Check Procedure

The primary calibration of the HCDM was performed at GCA. The two methods used for this purpose (known thickness absorber films, and CO_2-air mixtures) have been discussed previously in this report. Under field conditions, however, a simplified calibration checkout procedure was required. Such a secondary calibration is effected by inserting a partial obstruction of known characteristics into the beta source-detector gap, in order to simulate the presence of dust in a controlled manner.

This calibration check is performed as follows. The upper inlet plate is removed (after removal of three screws), and a cylindrical calibration tube is

lowered into the inlet duct, down to the beta sensing gap. This cylinder has a flange at this upper end which then rests (indexed by three pins) on the upper surface of the sample inlet flow duct (see Figure 2). The lower end of the metal cylinder has a slot-shaped window that reduces the radiation reaching the detector by reducing its field of view. The count reduction when inserting this window is about 25 percent (75 percent transmission). It was considered that this approach was entirely satisfactory as a check of the HCDM operation, in combination with the zero-concentration point obtained when purging the instrument.

In order to perform this secondary calibration check, the HCDM is operated in its usual manner, in a relatively clean (low dust concentration) environment, such as an office, or even a nondusty area of a mine. After the initial zero-check cycle, the above described calibration cylinder is inserted into the inlet duct and subsequent readings are noted. These readings should be within a few percent of the value marked on the calibration cylinder at the factory. After removing this calibration unit, the readings of the HCDM should return to zero. In this manner, a two-point calibration check is performed, fully characterizing the instrument operation.

SECTION 5

FINAL HCDM TESTING

Final testing of the HCDM prototype to be delivered to the U.S. Bureau of mines was performed after the unit was completed, all modifications had been implemented, and the wire wrap electronic component board had been replaced by the printed circuit board.

After the preliminary and rather superficial tests described previously, the device was subjected to a more systematic series of trials whose objective was to determine any operational abnormalities, both short-term as well as long-term. The tests included a complete characterization of the beta counting stability, dependence of this count rate on high-voltage supply fluctuations, count-rate drifts, etc. Subsequently, overall environmental tests were performed to assess any effect associated with temperature and/or humidity. Finally, dust, CO_2-air, and film absorber calibrations were carried out on the completed unit before its delivery to the Bureau.

Geiger Tube High Voltage Tests

The first series of tests focused on observed instabilities in the beta count rate significantly in excess of predicted statistical variations. Excessive deviations in both consecutive measurements and long-term drift (8 percent in 10 minutes) were observed for the original detector.

The pulse detector-counter circuit, analyzed on an oscilloscope and with a function generator, was found to perform normally. The software timing and counting functions were checked with a stable signal generator and no problems were encountered.

Two sources of beta count rate instability were then identified: (1) operation of the GMT at or near the high end of its plateau region, and (2) electrical characteristics of the GMT deviating from manufacturers specifications (i.e., excessive plateau slope).

It was observed that operation at 950 V brought the tube near the nonlinear region significantly degrading performance. The high voltage supply was then adjusted down to 910 volts, i.e., closer to the mid-portion of the plateau, and performance improved accordingly.

Long-term instability (drift) was found to be caused by excessive GM tube sensitivity to high-voltage supply output variations. Figure 29 shows the

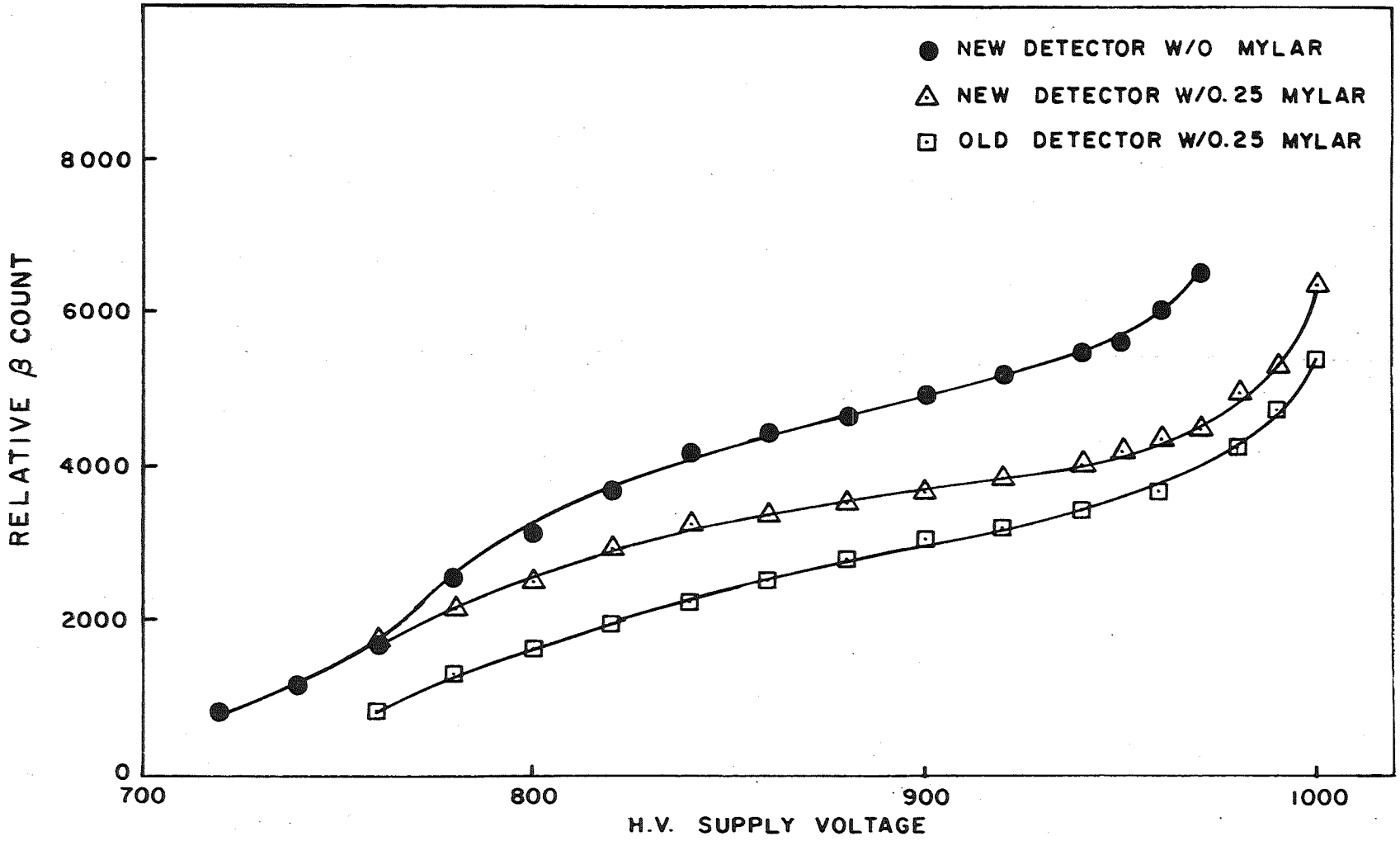


FIGURE 29. - Beta count rate vs voltage for two detectors.

observed beta count rate vs high voltage for two typical detectors. Plateau slopes of 37 percent/100 V and 21 percent/100 V compare poorly to the manufacturers spec of 5 percent/100 V. The high voltage supply of the HCDM was found to vary typically by ± 3 percent. This value was within the original specification, but inadequate for these detectors.

The high voltage power supply regulation circuit was redesigned by inclusion of a "varistor" in order to improve its regulation to within ± 0.1 percent over the range of applicable battery voltage changes. This modification resolved completely the above mentioned drift problem. Tests performed before the high voltage circuit redesign indicated a drift that was particularly noticeable during an initial warm up period of the order of 10 to 15 minutes. Although this warmup period would have been operationally acceptable, it was symptomatic of the more general problem of high voltage drift. Figures 30-32 show the mass concentration readings obtained at various simulated concentrations obtained by insertion of a partial obstruction within the beta sensing gap, before improvement of the high voltage circuit. Corresponding tests performed after that redesign show no discernible drift whatsoever.

Instrument Calibration Tests

Final HCDM calibration tests were performed by several alternative methods: insertion of thin films of known mass/area, CO_2-air mixtures, and dust.

a) Thin film calibration results.

Instrument calibration was performed using 0.15 mil and 0.30 mil (3.8 and 7.6 m) thickness mylar film absorbers to simulate mass concentrations of 475 g/m^3 and 950 g/m^3, respectively. Figure 33 shows the semilog response lines thus obtained. With the addition of a 0.25 mil mylar attenuator over the source, essentially semi-log linear (i.e., truly exponential) attenuation was therefore observed up to and including an equivalent concentration of 950 g/m^3, almost twice the maximum range for which the HCDM has been designed.

b) CO_2-air calibration.

A modified test set up for the CO_2-air mixture method of calibration was used for the final calibration of the prototype HCDM. As was described previously in this report, a noticeable departure from the exponential attenuation behavior had been observed when the clean-air curtain flow was not mixed with CO_2. It was suspected that this deviation resulted from the flow idiosyncracies of the experimental set up used to obtain those data, i.e., a variable degree of mixing between the two streams may have caused the apparent semi-log nonlinearity of the system response. A new calibration configuration was thus assembled providing improved flow control. This set up is depicted in Figure 34. Both conditions were evaluated, i.e., CO_2-air constrained to the central part of the sensing gap, and CO_2-air mixture throughout the entire gap. The data of Figure 35 indicate that the effective gap, with the clean air curtains in operation is about 1.6 cm and that the effective mass

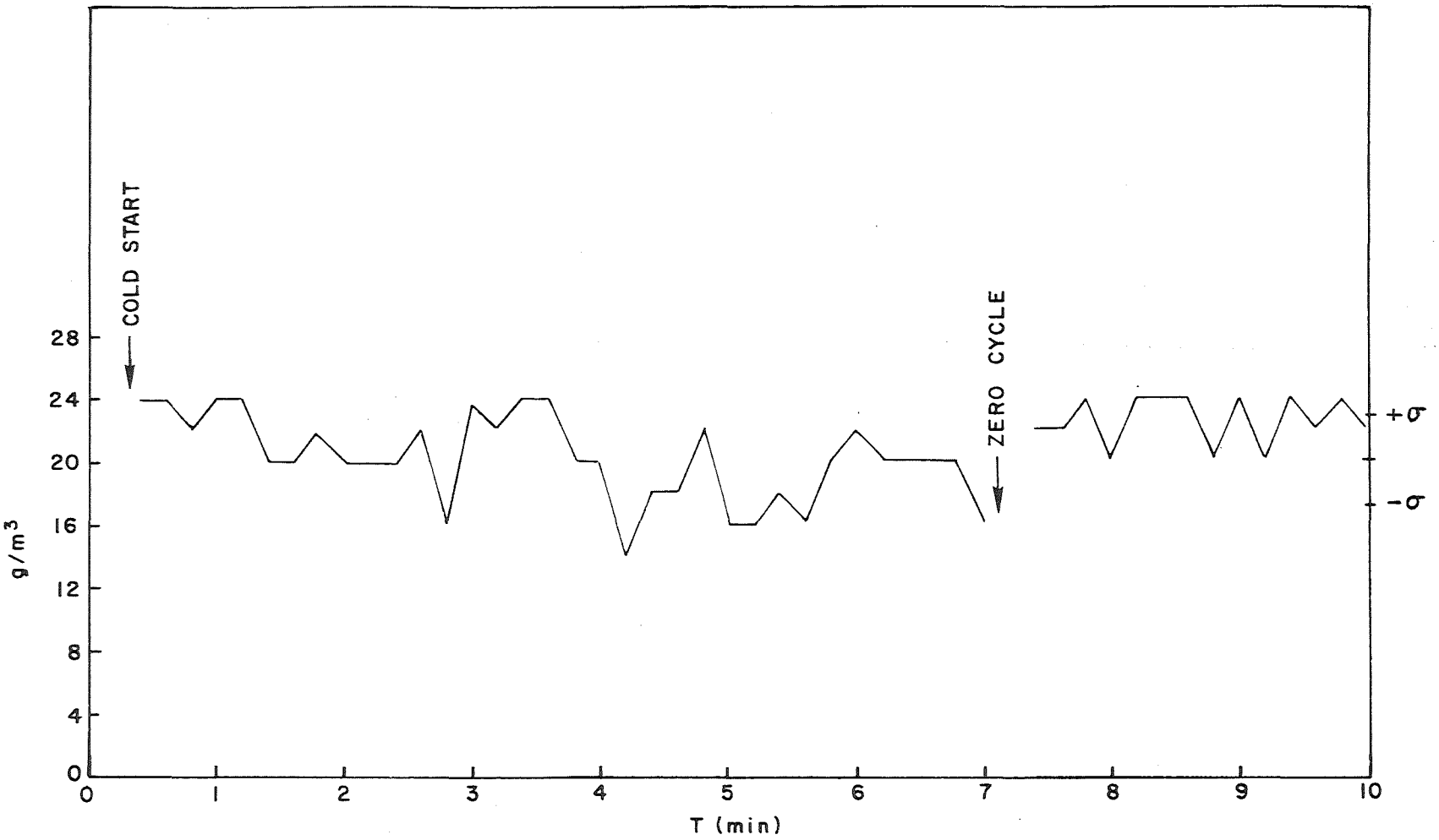


FIGURE 30. - Mass readouts for simulated concentration of 20 g/m^3 (data obtained before modification of the detection high voltage power supply circuit).

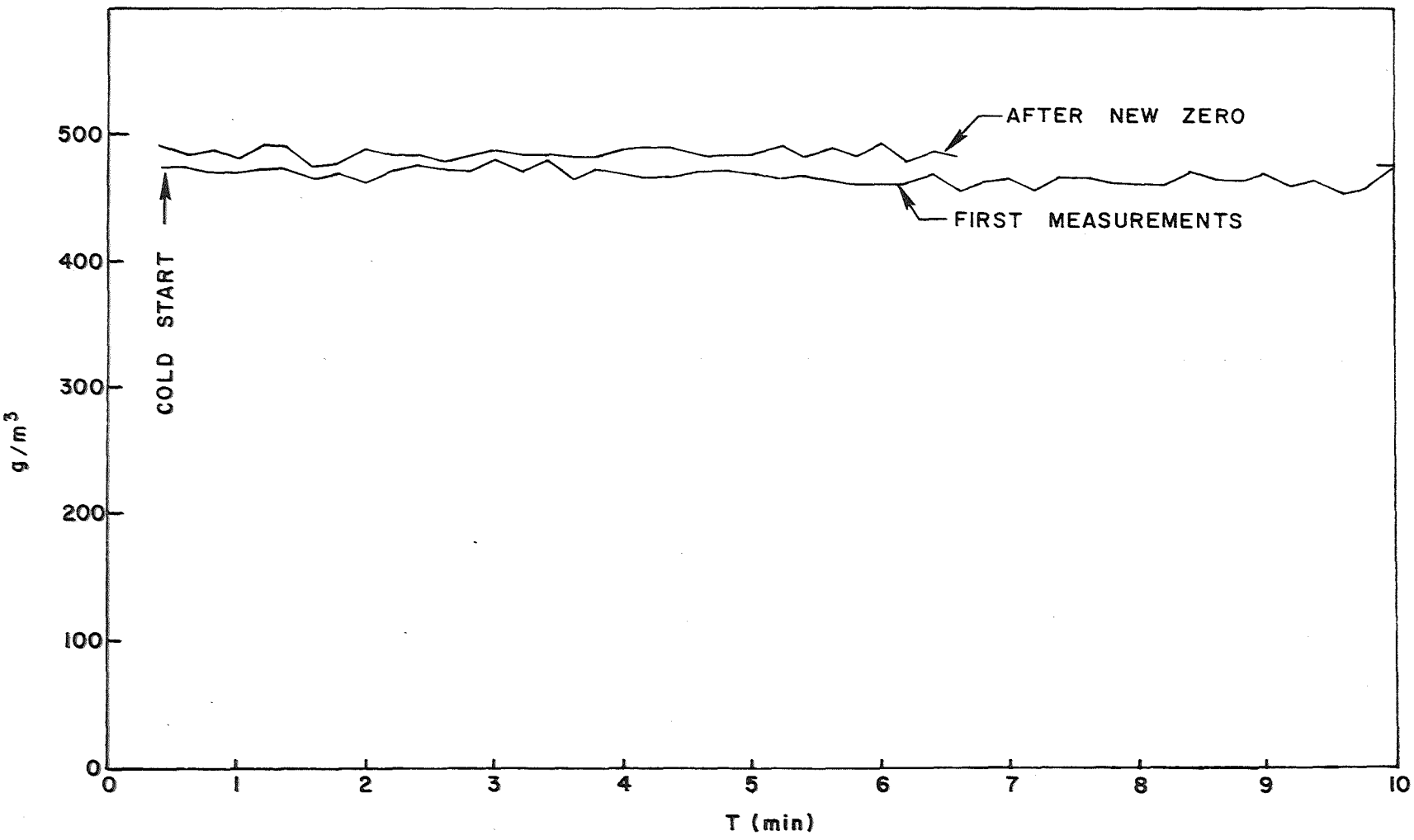


FIGURE 31. - Mass readout for equivalent concentration of 475 g/m^3 (data obtained before modification of the detector high voltage power supply circuit).

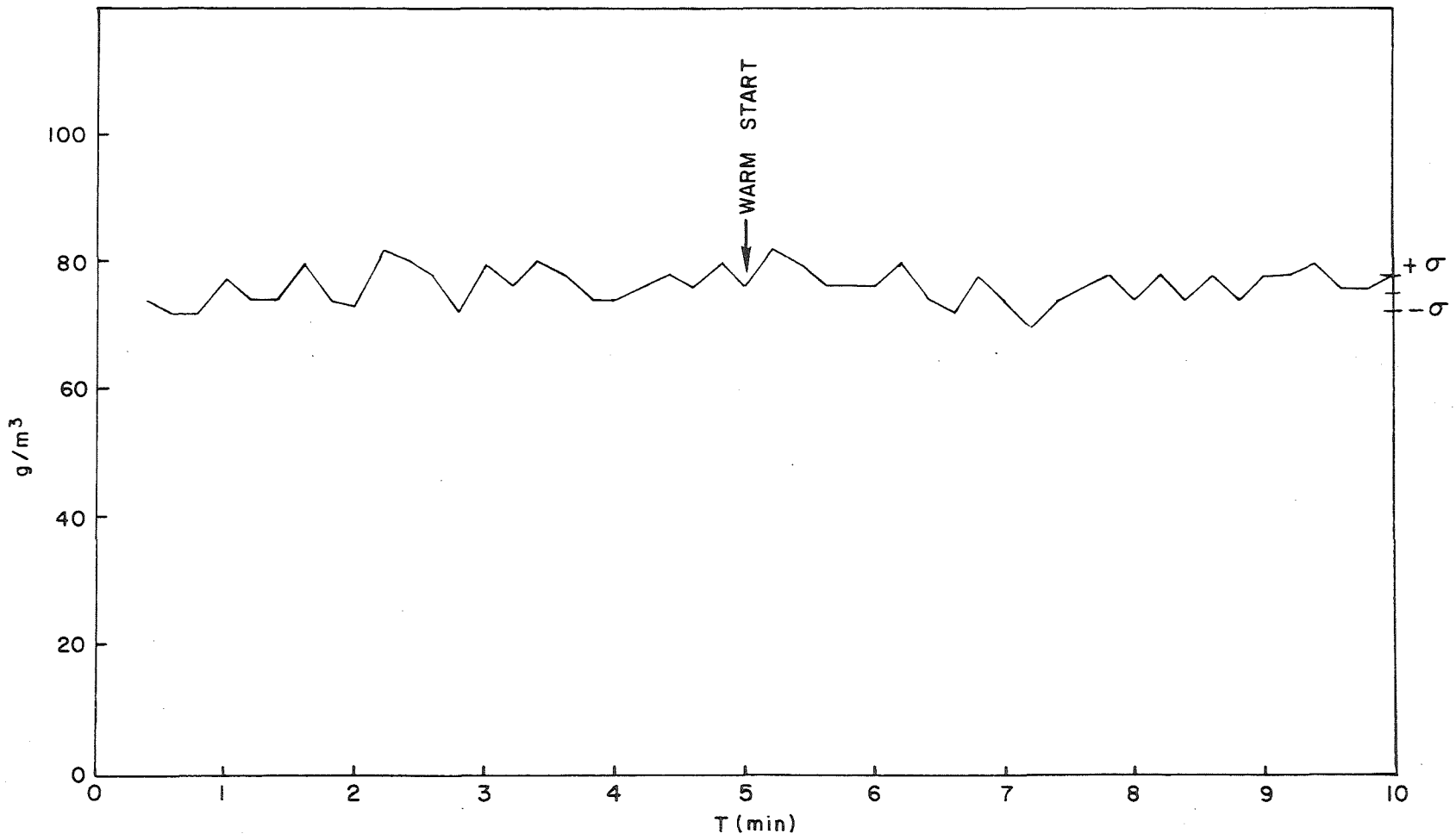


FIGURE 32. - Mass readouts for simulated concentration of 75 g/m^3.

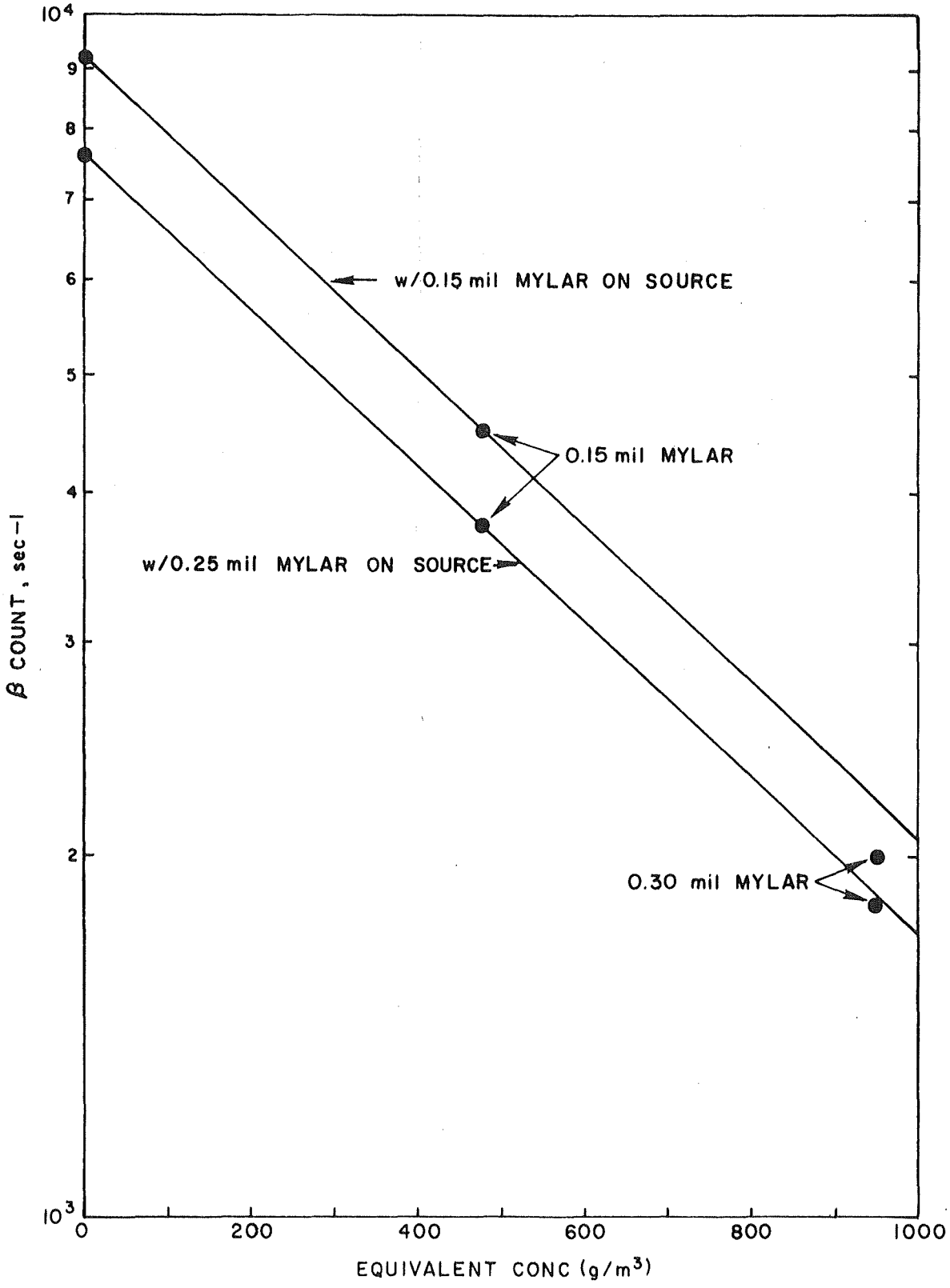


FIGURE 33. - Calibration of HCDM using Mylar absorbers.

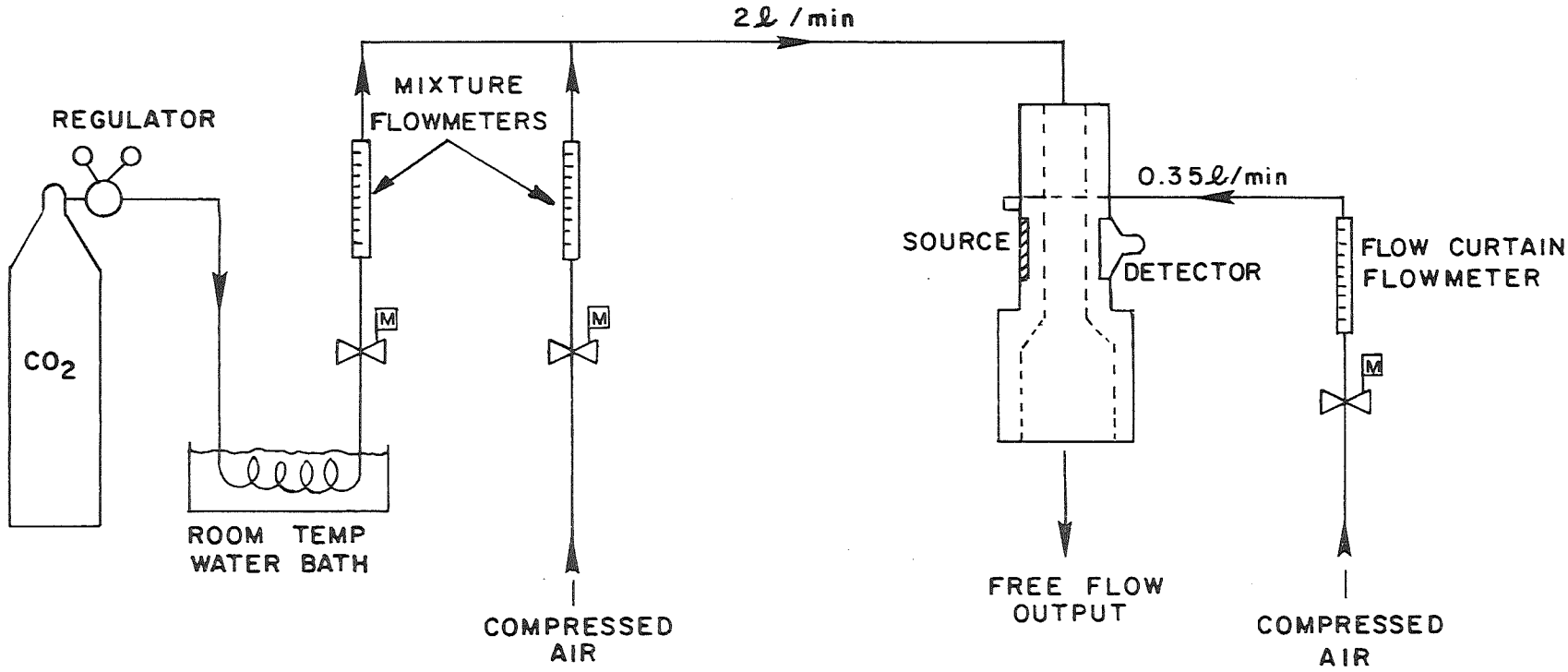


FIGURE 34. - Final CO_2-air calibration set up.

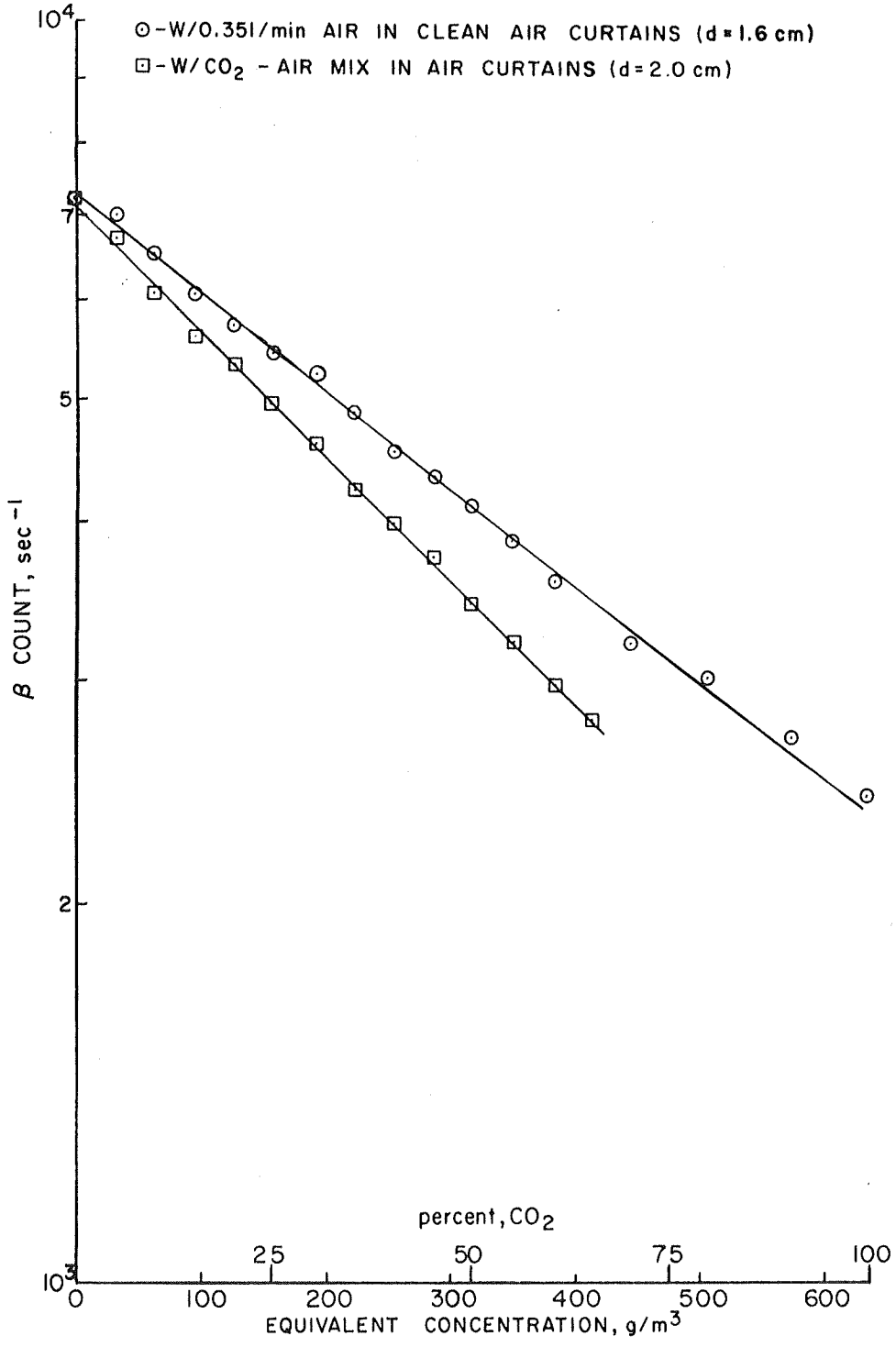


FIGURE 35. - CO_2-Air calibration results.

absorption coefficient, μm, of the sensing system is about 1.1 cm^2/mg. This value, in combination with the effective sensing gap, determines the calibration constant of the instrument, which is entered into the microprocessor memory.

c) Dust calibration.

Tests were performed with the HCDM to determine its response to the variable for which it was designed, i.e., airborne dust mass concentration. Considerable difficulties were encountered, as expected, in generating the extremely high concentration of dust required to evaluate and/or calibrate the HCDM. Three methods of generation were tried: a) using a vibrating sifter directly coupled to the inlet of the HCDM, b) using an elutriation tube with a high upward directed flow rate, and c) a combination of food blender and elutriation tube.

At any concentration exceeding about 10 to 20 g/m^3 clumping of the dust became a problem for all three methods of generation. Whenever such agglomeration occurred, the HCDM readings were consistently lower than the concentration values obtained by gravimetry of the high capacity filter downstream of the sensing region.

When clumping of the dust occurs, the speed of these large agglomerated particles significantly exceeds that of the air stream and since the HCDM senses the instantaneous concentration in the gap, particle velocity affects that response when compared to the concentration calculated from the gravimetric collection which is based on the sampling flowrate. In other words, the gravimetric reference technique is valid only if the air stream velocity and the dust velocity are identical. The beta mass sensing configuration senses the true instantaneous concentration which is, of course, the parameter of interest.

Up to about 10 or 12 g/m^3 the agreement between the HCDM readings and the gravimetrically determined concentration was quite acceptable, as shown in Figure 36. However, at higher concentrations, the readings obtained by the HCDM did not follow the concentration values obtained gravimetrically indicating that the truly aerosolized fraction of the dust did not increase significantly and that most of the dust being collected on the filter was in the form of clumps.

In summary, the CO_2-air calibration method (or using any other gas with similar properties) has proved to be extremely useful to generate the equivalent of very high aerosol concentrations, and provides a true absolute reference for the calibration of the HCDM.

Zero Concentration Stability Tests

An important operational parameter of the HCDM is the stability of the beta count rate as a function of time. A series of tests was performed to determine that long-term stability.

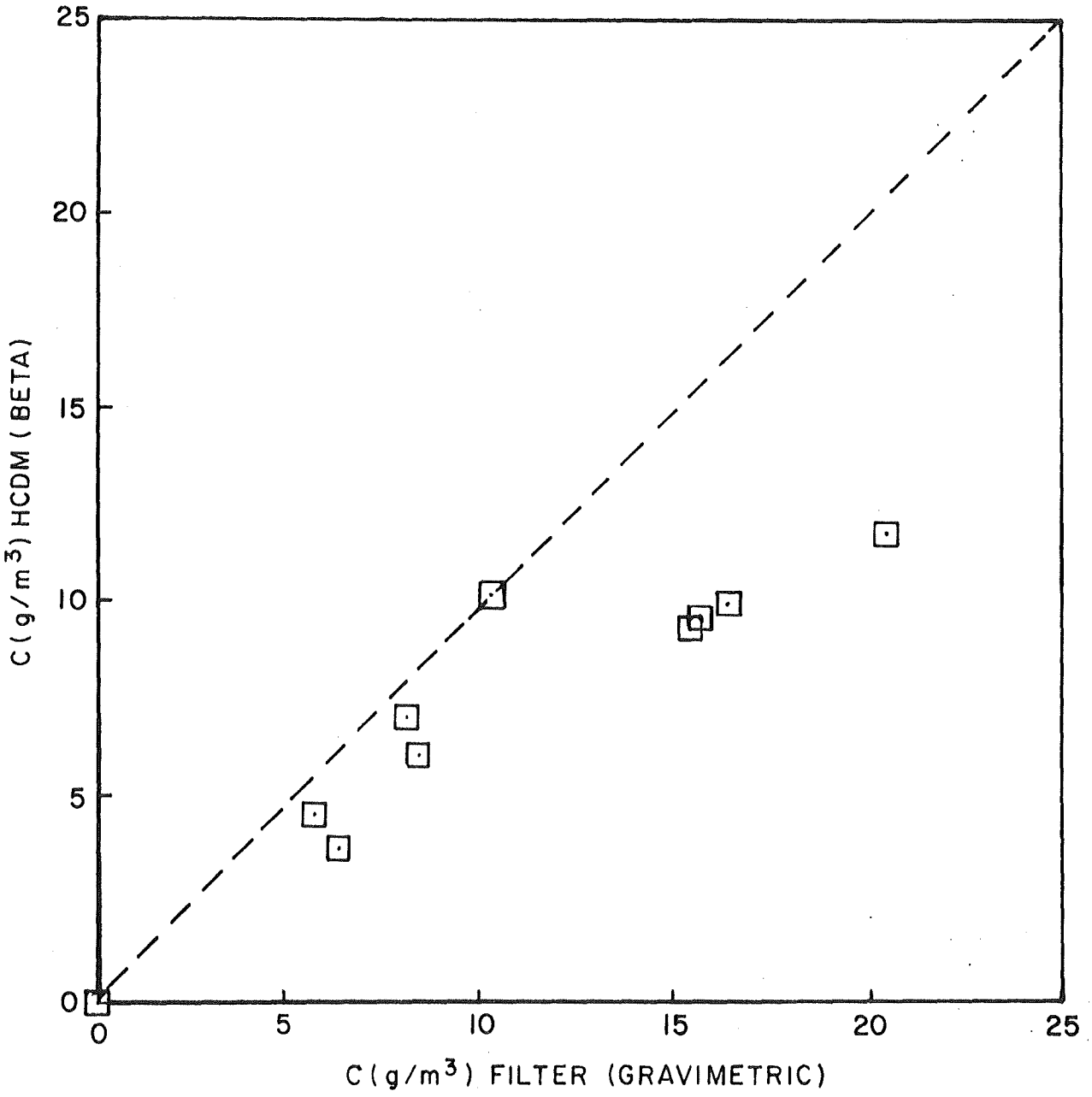


FIGURE 36. - Dust comparison tests.

Zero cycle beta counts and 10-second beta counts at 0 g/m^3 were recorded for two 12-hour periods. Figure 37 shows the percentage change over these periods. The largest drift, +1.1 percent/hour, corresponsds to -7 g/m^3 per hour, or only 0.7 g/m^3 between zero cycles.

The zero-concentration cycle rate (purge cycle) was checked for offset from the sampling count rate at 0 g/m^3. This was determined by running the HCDM in a clean environment and recording any systematic shift of the readings with respect to the zero-reference value. The zero cycle showed an average +0.2 percent deviation, or an offset of +1.1 g/m^3 in the concentration measurements, which is an acceptable error.

Statistical Measurement Error Determination

The ultimate limitation of the beta mass sensing technique is given by the random nature of the beta radiation process, as discussed in the initial section of this report. It was considered important, therefore, to determine experimentally the intrinsic variability of the measurements by establishing a fixed attenuation in the beta sensing gap. These tests were performed several times during the development of the HCDM in order to ascertain the proper operation of the device as it was being modified and optimized. Furthermore these serve to establish the normality of the Geiger detector's behavior.

The final tests to determine the standard deviation of the mass concentration readings obtained with the HCDM are summarized in the following table.

Simulated mass concentration (g/m^3)	58	312	470
Measured relative standard deviation (%)	4.1	1.1	0.65
Theoretical predicted rel. stand. dev. (%)	6.9	1.4	1.0

The above tabulated results indicate that the statistical fluctuations of the beta counting system of the HCDM are well within the predicted values and that the actual standard deviation at the minimum concentration of 20 g/m^3 should be of the order of 2.5 to 3.0 g/m^3 corresponding to a relative standard deviation of 12.5 to 15 percent, i.e., about one-half of the contractually stipulated value of 25 percent.

Environmental Testing Results

Environmental tests of the HCDM were performed in a large (1 m^3) controlled environment test chamber capable of providing a representative range of temperatures and humidities. The HCDM was placed inside this chamber and its output connected to an external digital printer which recorded the data every 10 seconds in real time.

The objective of these tests was to determine any effects resulting from temperature and humidity extremes as well as combinations of these two

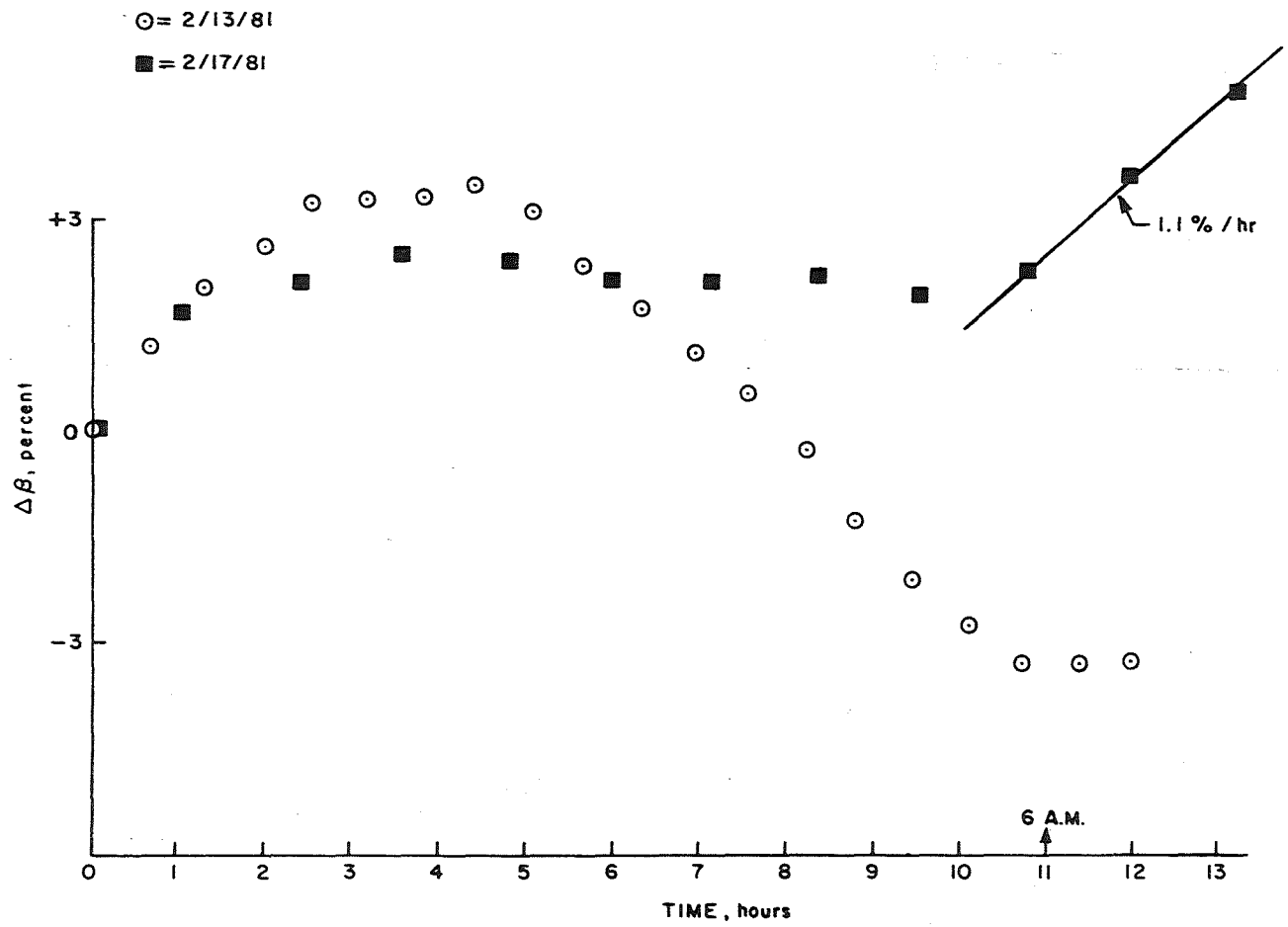


FIGURE 37. - Zero-concentration beta counting rate stability test results (without automatic zero-correction).

environmental parameters. Zero-concentration measurements were run continuously during these tests in order to determine any systematic temperature/humidity associated effects on the instrument operation. After each condition of temperature and humidity was allowed to stabilize, a series of 30 10-second readings was then recorded and the mean deviations from the average reading at 20°C and 40 percent (used as a reference condition) were calculated. These are presented in the following table, which also lists the corresponding values of the standard deviation for each of the 30 data blocks.

	Humidity		
	20%	40%	90%
Temperature			
0°C	$\Delta C = 0.4$ g/m^3 $\sigma = 1.96$ g/m^3	$\Delta C = -0.2$ g/m^3 $\sigma = 2.1$ g/m^3	
25°C	$\Delta C = +1.5$ g/m^3 $\sigma = 1.46$ g/m^3	$\Delta C = 0$ g/m^3 $\sigma = 1.65$ g/m^3	$\Delta C = +1.2$ g/m^3 $\sigma = 1.8$ g/m^3
40°C	$\Delta C = 0$ g/m^3 $\sigma = 1.44$ g/m^3	$\Delta C = -0.3$ g/m^3 $\sigma = 1.65$ g/m^3	$\Delta C = 0.8$ g/m^3 $\sigma = 1.4$ g/m^3

Upon inspection of the above table it can be concluded that there were no systematic temperature and/or humidity-related effects on the zero-readings of the HCDM prototype. The average of the deviations from the reference condition were all less than the standard deviation of the data points obtained for each environmental condition, i.e., steady-state environmentally-caused deviations are negligible with respect to the intrinsic random fluctuations of the beta counting rate. Time-varying temperature and/or humidity effects are, of course, expected and predictable as these influence the air density in the beta sensing gap, as discussed previously within this report.

CONCLUSIONS AND RECOMMENDATIONS

This development program has resulted in a prototype High Concentration Dust Monitor designed for fully self-contained mine-deployable operation.

The HCDM prototype constitutes a new type of instrument capable of sensing very high airborne dust concentrations by means of direct, real-time, beta radiation attenuation in air over the range of 20 to 500 g/m^3. This development should be considered a significant contribution to the state-of-the-art in dust monitoring instrumentation in that it incorporates several novel approaches and/or improvements over existing methods. Periodic automatic zero-concentration referencing, continuous protection of the sensing surfaces by clean air flows, the incorporation of a microprocessor designed to provide continuous recording of the data for subsequent playback and to control all functions of the instrument, and other operational features result in a very versatile device. Its application should transcend the originally intended coal mine monitoring purpose, extending to other potentially explosive environments such as grain loading and storage operations, power plant-related operations and sites (such as pulverizers and filter-baghouses), etc.

General applications for the HCDM include: the identification of hazardous conditions by measurement of dusts at explosive concentration levels above the lean flammable limit; conversely, the determination of safe conditions by measurements showing where dust concentrations are below hazardous levels; and the measurement of mass concentration of dense water mists and fogs. In addition, the HCDM may be applied to air and gas density determinations.

Forseeable in-mine uses are: monitoring at longwall face, or at transfer points where coal dust is not inerted by rock dust and, thus, may reach flammable concentrations.

It should be emphasized that the HCDM is designed to measure total mass concentration and, thus, the instrument should be used to assess flammability of either pure dusts or known mixtures of dust. Furthermore, and because of its mass sensing characteristic, the HCDM will not discriminate between dusts and other aerosols.

Although the laboratory tests performed with the HCDM prototype have been most successful, indicating performance that exceeds some of the original objectives, its definitive evaluation must be based on extensive field trials to be performed, among other locations, within the coal mine environment, under the demanding and extreme conditions prevailing near the mine face where the highest, and thus most dangerous concentrations of coal dust prevail. The requirement for any future design modifications, either in the hardware or the microprocessor program, will be contingent on the results and the experience derived from such field tests.

REFERENCES

1. Hertzberg, M., Cashdollar, K. L., and Lazzara, C. P., The Limits of Flammability of Pulverized Coals and Other Dusts, Eighteenth Symposium (International) on Combustion (Waterloo, Canada, August 17-22, 1980), The Combustion Institute, Pittsburgh, PA, 1981.

2. Palmer, K. N., Dust Explosions and Fires, Chapman and Hall, London, 1973.

3. Lilienfeld, P., Design and Operation of Dust Measuring Instrumentation Based on the Beta-Radiation Method. Staub Vol. 35, p. 458. 1975.

4. Cooper, D. W., Statistical Errors in Beta Absorption Measurements of Particulate Mass Concentration. J. Air Poll. Assoc. 25(11), 1975.

5. Liu, B. Y. H., and Pui, D. Y. H., Aerosol Sampling Inlets and Inhalable Particles, EPA-600/9-80-004, January 1980.

6. Zebel, G., Some Problems in the Sampling of Aerosols, in Recent Developments in Aerosol Science, D. T. Shaw, Ed., Wiley, New York, 1978.

7. Hastings, C., Approximations for Digital Computers, Princeton University Press, 1955.